







# Interferon lambda 4 can directly activate human CD19<sup>+</sup> B cells and CD8<sup>+</sup> T cells

Mairene Coto-Llerena<sup>1</sup>, Marco Lepore<sup>2</sup>, Julian Spagnuolo<sup>2</sup> , Daniela Di Blasi<sup>1,2</sup>, Diego Calabrese<sup>1</sup> , Aleksei Suslov<sup>1</sup>, Glenn Bantug<sup>3</sup>, Francois HT Duong<sup>1</sup>, Luigi M Terracciano<sup>4</sup>, Gennaro De Libero<sup>2,\*</sup> , Markus H Heim<sup>1,5,\*</sup> 

**Compared with the ubiquitous expression of type I (IFN $\alpha$  and IFN $\beta$ ) interferon receptors, type III (IFN $\lambda$ ) interferon receptors are mainly expressed in epithelial cells of mucosal barriers of the of the intestine and respiratory tract. Consequently, IFN $\lambda$ s are important for innate pathogen defense in the lung and intestine. IFN $\lambda$ s also determine the outcome of hepatitis C virus (HCV) infections, with IFN $\lambda$ 4 inhibiting spontaneous clearance of HCV. Because viral clearance is dependent on T cells, we explored if IFN $\lambda$ s can directly bind to and regulate human T cells. We found that human B cells and CD8<sup>+</sup> T cells express the IFN $\lambda$  receptor and respond to IFN $\lambda$ s, including IFN $\lambda$ 4. IFN $\lambda$ s were not inhibitors but weak stimulators of B- and T-cell responses. Furthermore, IFN $\lambda$ 4 showed neither synergistic nor antagonistic effects in costimulatory experiments with IFN $\lambda$ 1 or IFN $\alpha$ . Multidimensional flow cytometry of cells from liver biopsies of hepatitis patients from IFN $\lambda$ 4-producers showed accumulation of activated CD8<sup>+</sup> T cells with a central memory-like phenotype. In contrast, CD8<sup>+</sup> T cells with a senescent/exhausted phenotype were more abundant in IFN $\lambda$ 4-non-producers. It remains to be elucidated how IFN $\lambda$ 4 promotes CD8 T-cell responses and inhibits the host immunity to HCV infections.**

DOI 10.26508/lsa.201900612 | Received 25 November 2019 | Revised 26 October 2020 | Accepted 26 October 2020 | Published online 6 November 2020

## Introduction

Hepatitis C virus (HCV) is a parenteral transmitted hepatotropic virus that chronically infects an estimated 71 million persons worldwide (WHO, 2017). In most patients, chronic hepatitis C (CHC) leads to some degree of liver fibrosis and in 15–25% cirrhosis develops after 10–40 yr (Lauer & Walker, 2001). Patients with CHC and cirrhosis are at increased risk for liver failure and for developing hepatocellular carcinoma (El-Serag, 2012). Acute HCV infections are often oligo-

asymptomatic (Santantonio et al, 2008). In 70–80% of infected patients, the virus persists and the infection becomes chronic. Clearance of HCV in the acute phase depends on strong and sustained CD4<sup>+</sup> and CD8<sup>+</sup> T-cell responses against multiple peptides within different HCV proteins (Missale et al, 1996; Diepolder et al, 1997; Cooper et al, 1999; Lechner et al, 2000; Takaki et al, 2000; Thimme et al, 2001, 2002). The most direct evidence for the central role of T cells comes from depletion experiments with experimentally infected chimpanzees. Depletion of CD8<sup>+</sup> T cells before experimental infection of previously protected chimpanzees led to HCV persistence until CD8<sup>+</sup> T-cell response recovered and an HCV-specific CD8<sup>+</sup> T-cell response emerged (Shoukry et al, 2003). Furthermore, depletion of CD4<sup>+</sup> cells in previously protected chimpanzees led to HCV persistence and the emergence of CD8<sup>+</sup> escape variants (Grakoui et al, 2003). Collectively, these findings suggested that CD4<sup>+</sup> T cells promote persistence of protective immunity, whereas virus-specific CD8<sup>+</sup> T cells primarily function as the key effectors.

There is a significant association between certain HLA class I (e.g., HLA-B27) and class II (e.g., DRB1\*1101) alleles and spontaneous elimination of the virus (Neumann-Haefelin & Thimme, 2013). However, the strongest predictor for spontaneous clearance is a genetic polymorphism in the IFN $\lambda$  gene locus (Thomas et al, 2009; Rauch et al, 2010; Tillmann et al, 2010). Initially described as the IL28B (IFN $\lambda$ 3) genotype, it has become clear that the originally identified single nucleotide polymorphism rs12979860 and rs8099917 are surrogate markers for the functional single nucleotide polymorphism rs368234815 located in exon 1 of IFN $\lambda$ 4 (Bibert et al, 2013; Prokunina-Olsson et al, 2013). The ancestral allele (designated the  $\Delta$ G allele) encodes a fully functional IFN $\lambda$ 4 protein, whereas the mutant TT allele encodes an inactive variant with a premature stop codon (Prokunina-Olsson et al, 2013). The impact of this genetic polymorphism on spontaneous clearance is striking: clearance occurs in 50–60% of patients homozygous for the mutant inactive allele, but in only 10–20% of patients with one or two functional alleles (Thomas et al, 2009; Tillmann et al, 2010; Terczynska-Dyla et al, 2014). The association between low spontaneous clearances of HCV with

<sup>1</sup>Department of Biomedicine, Hepatology, University Hospital and University of Basel, Basel, Switzerland <sup>2</sup>Department of Biomedicine, Experimental Immunology, University Hospital and University of Basel, Basel, Switzerland <sup>3</sup>Department of Biomedicine, Immunobiology, University Hospital and University of Basel, Basel, Switzerland <sup>4</sup>Molecular Pathology Division, Institute of Pathology, University Hospital Basel, Basel, Switzerland <sup>5</sup>Division of Gastroenterology and Hepatology, Clarunis, University Center for Gastrointestinal and Liver Diseases, Basel, Switzerland

Correspondence: markus.heim@unibas.ch; gennaro.delibero@unibas.ch  
\*Gennaro De Libero and Markus H Heim share co-senior authorship

the IFN $\lambda$ 4 “producer” genotype is statistically significant, but mechanistically unexplained. Conceptually, the simplest mechanistic model predicts that (1) HCV-infected hepatocytes produce and secrete IFN $\lambda$ 4, and (2) IFN $\lambda$ 4 binds to one or more types of immune cells and inhibits the cellular immune response that is critical for HCV clearance. Presently, both assumptions are not supported by direct evidence. So far, IFN $\lambda$ 4 protein could not be detected in liver biopsies of patients with HCV infections. Nevertheless, there is strong indirect evidence that IFN $\lambda$ 4 is a key driver of innate immune responses in HCV infection (Terczynska-Dyla et al, 2014; Heim et al, 2016). The second assumption is also controversial. IFN $\lambda$  signals through a receptor composed of the ubiquitously expressed IL10RB chain (shared with the IL-10 receptor) and a unique IFN $\lambda$  receptor chain (IFN $\lambda$ R1) whose expression is mainly restricted to epithelial cells (Kotenko et al, 2003; Donnelly et al, 2004; Sommereyns et al, 2008; Hamming et al, 2013). There are conflicting reports whether human lymphocytes express IFN $\lambda$ R1 and respond directly to IFN $\lambda$  (Gallagher et al, 2010; Dickensheets et al, 2013). However, there is increasing evidence that IFN $\lambda$  has immunomodulatory effects on T cells. During acute lymphocytic choriomeningitis virus (LCMV) infection, IFN $\lambda$  receptor (IFN $\lambda$ R)-deficient mice had increased expansion of CD4 $^{+}$  and CD8 $^{+}$  T cells and enhanced T-cell responses to LCMV re-challenge (Misumi & Whitmire, 2014). These findings led to the hypothesis that IFN $\lambda$  inhibits T-cell responses. However, because IFN $\lambda$ R could not be detected on T cells and IFN $\lambda$ R-deficient T cells did not respond better than wild-type T cells when transferred in acutely infected WT mice, the authors concluded that the effects on T cells occurred indirectly as a result of IFN $\lambda$  effects on other cell types (Misumi & Whitmire, 2014).

There is also evidence that IFN $\lambda$  regulates humoral immune responses, although controversial data were reported in different experimental approaches. Pretreatment of PBMCs from healthy volunteers with IFN $\lambda$ 3 reduced IgG secretion induced by stimulation with H1N1 Influenza virus (Egli et al, 2014). Another study conducted in a mouse vaccination model indicated that IFN $\lambda$ 3 increased vaccine-specific antibody production and IFN $\gamma$  release (Morrow et al, 2009). A stimulatory effect of IFN $\lambda$  on antibody production was confirmed in a more recent investigation (Ye et al, 2019). Of note, IFN $\lambda$  had no direct effect on B cells in mice but acted indirectly by stimulating the secretion of thymic stromal lymphopoietin (TSLP) by M cells in the upper airways. TSLP, in turn, stimulated dendritic cells and boosted immunoglobulin production (Ye et al, 2019). Yet another study found no difference in antibody production between wild-type and IFN $\lambda$ R-deficient mice (Misumi & Whitmire, 2014). In humans, IFN $\lambda$  might regulate B cells through a direct interaction (de Groen et al, 2015). IFN $\lambda$ R1 was found to be expressed in naive B cells at a very low level (de Groen et al, 2015). Furthermore, stimulation of naive human B cells with IFN $\lambda$ 1 induced IFN stimulated genes (ISGs) and enhanced TLR7/8-induced Ig production (de Groen et al, 2015).

Here we investigated the capacity of major human circulating immune cell populations to directly respond to IFN $\lambda$  and explored different functional outcomes in responsive cells. Finally, we used multicolor flow cytometry of liver infiltrating lymphocytes to compare T-cell subpopulations in patients with different IFN $\lambda$ 4 genotypes.

## Results

### Human B cells and CD8 $^{+}$ T cells are responsive to IFN $\lambda$

The responsiveness of human immune cells to direct IFN $\lambda$  stimulation is poorly characterized (Sommereyns et al, 2008). Therefore, we investigated whether circulating cells from healthy individuals were sensitive to IFN $\lambda$ , by monitoring IFNLR-mediated phosphorylation (i.e., activation) of signal transducer and activator of transcription 1 (STAT1). Treatment with IFN $\lambda$ 1 induced STAT1 phosphorylation in PBMCs purified from three healthy donors, albeit at lower levels than the control stimulation with IFN $\alpha$  (Fig 1A). Longer incubation times or higher doses of IFN $\lambda$ 1 did not increase the level of STAT1 phosphorylation (Fig 1B), suggesting that the overall lower response to IFN $\lambda$ 1 could be due to differential IFNLR expression patterns within individual PBMC populations. We determined the responsiveness to IFN $\lambda$ 1 of distinct cell subsets isolated from PBMCs, including total CD3 $^{+}$  T cells, or sorted CD4 $^{+}$  or CD8 $^{+}$  T cells, sorted CD19 $^{+}$  B cells, CD14 $^{+}$  monocytes, and CD3 $^{+}$ /CD16 $^{+}$  NK cells. IFN $\lambda$ 1-induced STAT1 phosphorylation (pY-STAT1) was detected in B cells and CD8 $^{+}$  T cells, whereas it was virtually absent in CD14 $^{+}$  cells and in NK cells (Fig 1C). In CD4 $^{+}$  T cells, the pY-STAT1 signal was already detectable in untreated samples, and did not increase upon IFN $\lambda$ 1 stimulation (Fig 1C), suggesting a lack of responsiveness of this subset. Thus, B cells and CD8 $^{+}$  T cells were the only responders to IFN $\lambda$ 1 among PBMC major subsets, and they were probably responsible for the weak signal observed in total PBMCs after IFN $\lambda$ 1 stimulation. Interestingly, both cell populations also responded to IFN $\lambda$ 4 (Fig 1D).

We next determined the gene expression levels of the two components of the type III IFN receptor, namely IFNLR1 and IL10RB, in purified immune cell populations. Consistent with their sensitivity to IFN $\lambda$ 1 and IFN $\lambda$ 4, B and CD8 $^{+}$  T cells displayed higher expression levels of IFNLR1 and IL10RB genes as than the other cell subsets (Fig 1E), whereas the expression of IL10RB and IFNAR1 was comparable in all the cell populations (Fig 1E).

Taken together, these results indicated that the unique capacity of human B cells and CD8 $^{+}$  T cells to respond to IFN $\lambda$  stimulation might be related with the IFNLR1 gene expression levels found in these cell populations.

### Neutrophils are responsive to IFN $\lambda$

Recently, neutrophils have emerged as significant target of IFN $\lambda$  (Rivera, 2019) expressing functional IFNLR1 and responding to IFN $\lambda$  stimulation *ex vivo* by activation of STAT1 phosphorylation (Blazek et al, 2015). In accordance with these reports, IFN $\lambda$ 1 induced of STAT1 phosphorylation in neutrophils isolated from two healthy donors (Fig S1A). Similar to PBMCs (Fig 1A), IFN $\lambda$ 1-induced STAT1 phosphorylation was weaker than IFN $\alpha$  (Fig S1A). IFN $\lambda$ 1 and IFN $\lambda$ 4 showed a weak stimulatory effect on neutrophil migration on their own and did not interfere with fMLP (N-formyl-L-methionyl-L-leucyl-phenylalanine)-induced neutrophil migration (Fig S1B).

### IFN $\lambda$ 4 does not enhance or interfere with TLR-mediated early B-cell activation

We next investigated the impact of IFN $\lambda$  stimulation on the functional properties of both B cells and CD8 $^{+}$  T cells. We first focused on

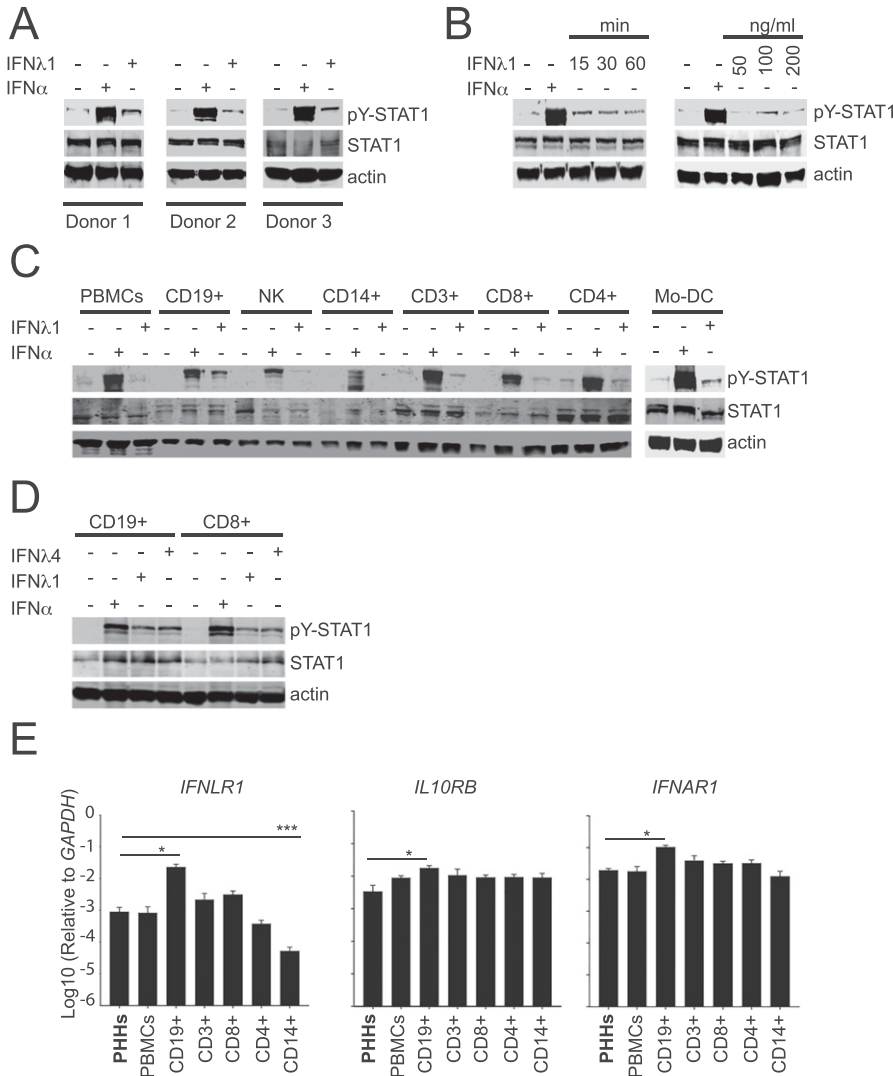


**Figure 1. Identification of IFN- responsive cell populations in PBMCs.**  
**(A)** PBMCs were stimulated for 15 min with 1,000 IU/ml IFN $\alpha$  or 100 ng/ml of IFN $\lambda$ 1. Western blot detection of phosphorylated STAT1 (pY-STAT1), total STAT1, and actin protein in total cell lysates of PBMCs obtained from three different donors. **(B)** Purified human PBMCs were stimulated with 100 ng/ml of IFN $\lambda$ 1 for 15, 30, and 60 min or 1,000 IU/ml of IFN $\alpha$  for 15 min (left panel) or with 50, 100, and 200 ng/ml of IFN $\lambda$ 1 or 1,000 IU/ml of IFN $\alpha$  for 15 min. Shown are representative blots from two different donors. **(A, C)** Total PBMCs and purified CD19 $^+$  B cells, CD3 $^+$  cells, CD8 $^+$  T cells, CD4 $^+$  T cells, CD3 $^+$ /CD16 $^+$  NK cells, and CD14 $^+$  monocytes were stimulated for 15 min with 1,000 IU/ml IFN $\alpha$  or 100 ng/ml IFN $\lambda$ 1 and analyzed as described in (A). A representative blot from two experiments is shown. **(A, D)** PBMC-derived CD19 $^+$  B cells and CD8 $^+$  T cells were stimulated for 15 min with 1,000 IU/ml IFN $\alpha$ , 100 ng/ml IFN $\lambda$ 1, or 100 ng/ml IFN $\lambda$ 4 and analyzed as described in (A). **(E)** qRT-PCR analysis of *IFNLR1*, *IFNAR1*, and *IL10RB* transcripts in total RNA isolated from the indicated PBMC subpopulations and primary human hepatocytes. Transcript levels are expressed as the  $\Delta\Delta$ CT relative to *GAPDH*. Results are shown as mean  $\pm$  SEM; n = 3.

B cells. According to published studies, both IFN $\alpha$  and IFN $\lambda$ 1 enhance B-cell responses to TLR ligands (Bekeredjian-Ding et al, 2005; de Groen et al, 2015). In contrast, the role of IFN $\lambda$ 4 in regulating B-cell activation is not known. Thus, we asked whether IFN $\lambda$ 4 could modulate B-cell functions. In a first series of experiments, purified CD19 $^+$  B cells were stimulated for 48 h with saturating doses of IFN $\alpha$ , IFN $\lambda$ 1, or IFN $\lambda$ 4 in the absence of TRL ligands and analyzed by flow cytometry for the expression of the early activation marker CD69. IFN $\alpha$  induced a marked and statistically significant increase in the frequency of CD69 $^+$ -activated B cells and of CD69 median fluorescence intensity (Fig 2A). IFN $\lambda$ 1 induced a slight but statistically significant increase, whereas IFN $\lambda$ 4 failed to promote a comparable response.

Of note, IFN $\lambda$ 4 did not alter the frequency of CD69 $^+$  B cells also when used in combination with IFN $\alpha$  or IFN $\lambda$ 1 (Fig 2B), thus suggesting lack of synergistic or antagonistic effect with IFN $\alpha$  and IFN $\lambda$ 1 on early B-cell stimulation. All three IFNs induced the expression of the ISGs *IFI27*, *Mx1*, *IFIT1*, and *OAS1* (Fig 2C). This finding confirmed that B cells may respond to IFNs and suggested that the differences between IFN $\alpha$  and IFN $\lambda$ s in regard to B-cell activation are not due to nonspecific differences in

signal transduction. Of note, no antagonism or synergism was observed between all IFNs in regard to ISG induction (Fig 2C).

We next investigated whether IFN $\lambda$ 4 stimulation could impact TLR-mediated activation of B cells. In agreement with previous studies (de Groen et al, 2015), IFN $\alpha$  and IFN $\lambda$ 1 significantly enhanced TLR-mediated early B-cell activation as measured by an increase in both frequency of CD69 $^+$  B cells and CD69 MFI (Fig 2D). Conversely, IFN $\lambda$ 4 had no effect on TLR9-dependent B-cell stimulation (Fig 2D), nor inhibited the B-cell stimulatory activity of IFN $\alpha$ , IFN $\lambda$ 1, or CpG (ODN2006) (Fig 2E). Collectively, these data suggested that the B cells responsiveness to IFN $\lambda$ 4 did not result in significant functional changes in the early B-cell activation program. Furthermore, IFN $\lambda$ 4 did not interfere with the capacity of IFN $\alpha$ , IFN $\lambda$ 1, or CpG (ODN2006) to stimulate early B-cell activation.

#### IFN $\lambda$ 4 is a weak inducer of IL-10 production by B cells

IL-10 is a potent inhibitor of cellular immune responses and is released by several cell types, including activated B cells (Blair et al,

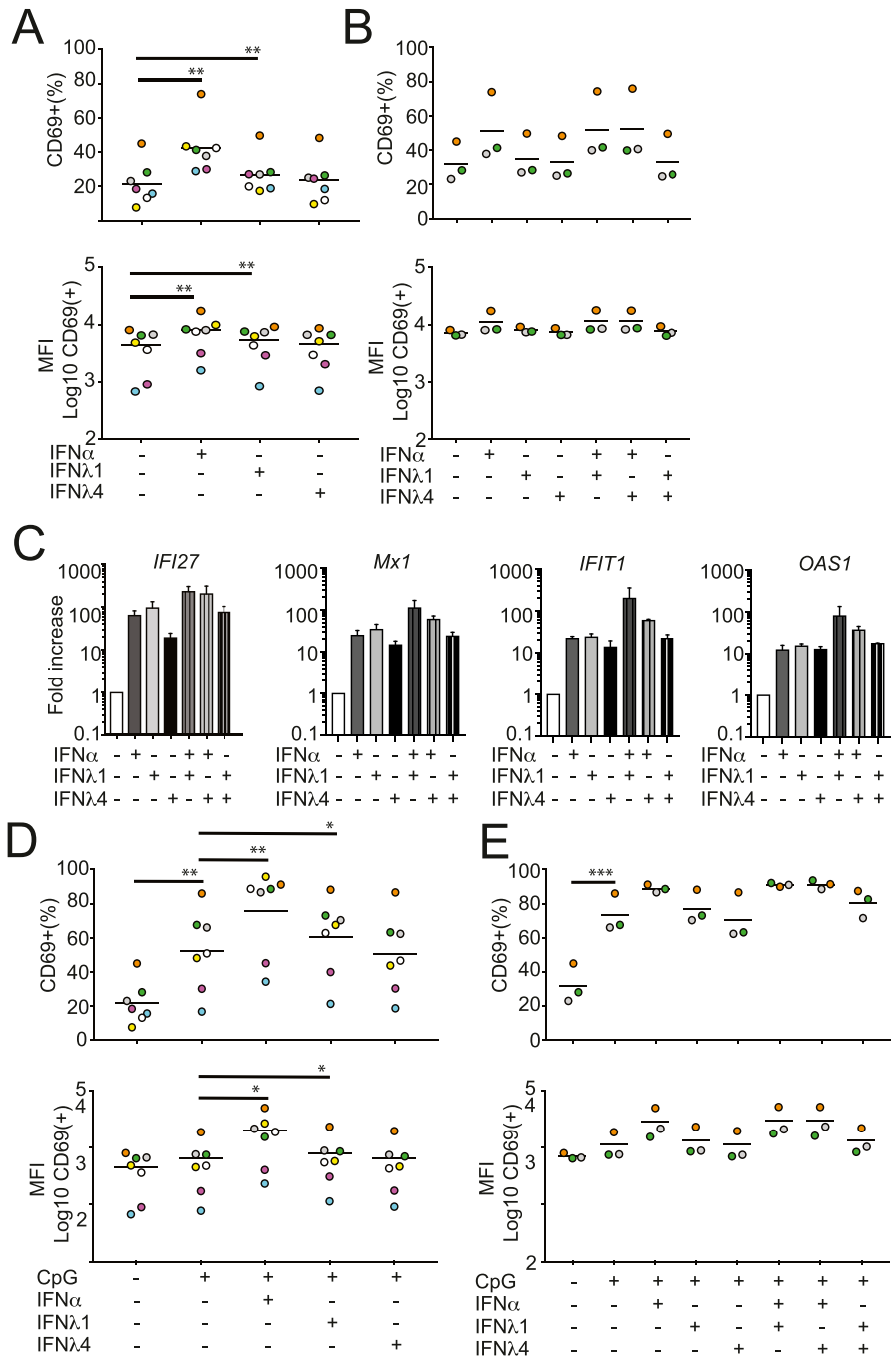


**Figure 2. IFN $\lambda$ 4 has no co-stimulatory activity on B-cell activation.**

B cells were isolated from PBMCs and stimulated with IFN and/or CpG ODN2006 for 48 h and analyzed for B-cell activation. **(A)** B cells isolated from seven donors were stimulated with IFN $\alpha$  (1,000 IU/ml), IFN $\lambda$ 1 (100 ng/ml) and IFN $\lambda$ 4 (100 ng/ml), fixed, and analyzed by CD69-specific mAbs by FACS. Percentages of CD69 $^{+}$  cells within the B-cell population (upper panel) or median fluorescence intensity (MFI) of CD69 $^{+}$  cells within the B-cell population (lower panel) are shown. Significant changes between IFN-treated and control samples are denoted by a thick line. **(A, B)** B cells isolated from three donors were stimulated with IFN $\alpha$  (1,000 IU/ml), IFN $\lambda$ 1 (100 ng/ml), and IFN $\lambda$ 4 (100 ng/ml) alone or in combination and analyzed as described in (A). Significant changes between IFN-treated versus single IFN treatment are denoted by a thick line. **(C)** *IFI27*, *Mx1*, *OAS1*, and *IFIT1* transcript levels in B cells stimulated with individual or combinations of IFN $\alpha$ , IFN $\lambda$ 1, and IFN $\lambda$ 4 were analyzed by qRT-PCR of total RNA. Results are shown as  $\Delta\Delta$ CT relative to *GAPDH* (mean  $\pm$  SEM; n = 2). **(D, E)** B cells were stimulated with IFN $\alpha$  (1,000 IU/ml), IFN $\lambda$ 1 (100 ng/ml), and IFN $\lambda$ 4 (100 ng/ml) alone (D) or in combination (E) in the presence or absence of CpG (0.8  $\mu$ g/ml). **(A)** Cells were analyzed as described in (A). **(A, B, D, E)** Colors depict individual donors and thin horizontal lines indicate the mean; n = 7 for (A) and (D); n = 3 for (B) and (E). \**P* < 0.05, \*\**P* < 0.01, and \*\*\**P* < 0.001 (paired *t* test).

2010; Das et al, 2012). High levels of IL-10 have been linked with immune-suppression in multiple chronic infections, including HCV (Lund, 2008; Ng & Oldstone, 2014). We hypothesized that IFN $\lambda$ 4 stimulation could promote IL-10 secretion by activated B cells. CD19 $^{+}$  enriched B cells were stimulated for 48 h with IFNs in the presence or absence of CpG (ODN2006), a TLR9 ligand. Culture supernatants were then analyzed for IL-10 protein levels by ELISA. In the absence of TLR9 triggering, IFNs did not induce IL-10 secretion by B cells (Fig 3A). When individually combined with CpG (ODN2006), all IFNs promoted a significant increase in IL-10

production, with IFN $\lambda$ 4 being the weakest stimulator (Fig 3A). Interestingly, we did not find any synergistic or antagonistic effect of IFN $\lambda$ 4 when used in combination with IFN $\lambda$ 1 or IFN $\alpha$  (Fig 3A). In agreement with previous studies (Banko et al, 2017), the CD19 $^{+}$ /CD27 $^{+}$  B cells, which are enriched in the memory B-cell population, were the main source of IL-10 upon stimulation with CpG and IFN $\lambda$ 1 or IFN $\lambda$ 4 (Fig 3B).

Another effect of TLR9 ligation in CD19 $^{+}$ /CD27 $^{+}$  memory B cells is induction of IgG release in the absence of B-cell receptor stimulation (Bernasconi et al, 2003). This response was not significantly

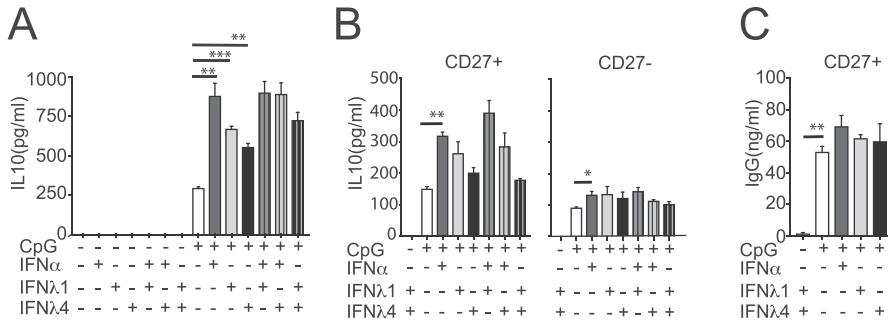


**Figure 3. IFNλ4 induces IL-10 production in B cells.** (A) B cells (n = 4) were stimulated with IFNα (1,000 IU/ml), IFNλ1 (100 ng/ml), and IFNλ4 (100 ng/ml) alone or in combination and in the presence or absence of CpG (2.5 μg/ml) for 48 h. Cell supernatants were collected and released IL-10 was determined by ELISA. Results shown as ± SEM from two independent experiments. Significant changes between IFN-treated and control samples as well as IFN combinations versus single IFN treatment are denoted by a thick line. (B) Memory (CD27<sup>+</sup> CD19<sup>+</sup>) and naïve (CD27<sup>-</sup> CD19<sup>+</sup>) B cells were stimulated with IFNα (1,000 IU/ml), IFNλ1 (100 ng/ml), and IFNλ4 (100 ng/ml) alone or in combination for 48 h either in the absence or presence of CpG (2.5 μg/ml). IL-10 present in supernatants of TLR9-stimulated and unstimulated cells in the presence of IFN was analyzed by ELISA. Results show mean ± SEM concentration (n = 4). (C) Memory B cells were treated with IFNα (1,000 IU/ml), IFNλ1 (100 ng/ml) or IFNλ4 (100 ng/ml) in the presence of CpG (2.5 μg/ml) for 48 h. The presence of IgG in the supernatants of stimulated and unstimulated controls was analyzed by ELISA. Results show the mean ± SEM concentration (n = 4). \*P < 0.05, \*\*P < 0.01, and \*\*\*P < 0.001 compared with the control condition (paired t test).

unstimulated cells in the presence of IFN was analyzed by ELISA. Results show mean ± SEM concentration (n = 4). IFNλ1 (100 ng/ml) or IFNλ4 (100 ng/ml) in the presence of CpG (2.5 μg/ml) for 48 h. The presence of IgG in the supernatants of stimulated and unstimulated controls was analyzed by ELISA. Results show the mean ± SEM concentration (n = 4). \*P < 0.05, \*\*P < 0.01, and \*\*\*P < 0.001 compared with the control condition (paired t test).

increased by IFNα or IFNλ1 (de Groen et al, 2015). We investigated whether IFNλ4 could modulate IgG production by CpG (ODN2006)-stimulated purified memory B cells. IFNλ4, like IFNα or IFNλ1 (de Groen et al, 2015), did not increase nor impair CpG (ODN2006)-induced IgG secretion (Fig 3C). Altogether, these data suggested that in memory B cells IFNλ4 promotes similar but less pronounced functional responses than those induced by other type III and type I IFNs.

**IFNλ4 enhances IFNγ production by TCR stimulated CD8 T cells**

Alike B cells, CD8<sup>+</sup> T cells showed response to IFNλ (Fig 1C). Thus, we asked whether IFNλ could modulate CD8<sup>+</sup> T-cell functions. Purified CD8<sup>+</sup> T cells were stimulated for 48 h with saturating doses of IFNλ1 or IFNλ4 in the presence or absence of titrating doses of plastic-bound anti-CD3 mAbs. Secreted IFNγ, a cytokine with potent antiviral activity, including HCV (Slifka & Whitton, 2000), was measured in culture supernatants as readout of response.

IFNλ1 and IFNλ4 did not trigger any IFNγ production by CD8<sup>+</sup> T cells in the absence of plastic-bound anti-CD3 mAbs (Fig 4A). Instead, they both significantly enhanced IFNγ secretion (2.94 ± 0.71 and 2.85 ± 0.38-fold, respectively) in the presence of suboptimal doses (0.1 μg/ml) of anti-CD3 mAbs (Fig 4A). Such synergistic effect with TCR-mediated stimulation was lost when higher doses of anti-CD3 mAbs were used (Fig 4A). Additional experiments with a fixed suboptimal dose of plastic-bound anti-CD3 mAbs and limiting doses of IFNλ1 or IFNλ4 confirmed a dose-dependent relation between the amount of IFNγ released by CD8<sup>+</sup> T cells and the concentrations of IFNλ1 or IFNλ4 (Fig 4B). Thus, both IFNλ1 and IFNλ4 enhance secretion of IFNγ by CD8<sup>+</sup> T cells in conditions of suboptimal TCR stimulation with anti-CD3 mAbs, which more closely resemble physiological antigen stimulation. Next, we investigated whether IFNλ has also synergistic effects on secretion of other cytokines by CD8<sup>+</sup> T cells (Fig 4C–H). IFNλ1 significantly stimulated IL-10 and IL-1β in anti-CD3-activated cells but had no significant impact on secretion of IL-22, GM-CSF, or TNFα.

CD8<sup>+</sup> T cells can be classified according to the differential expression of two surface markers (CD45RA and CCR7) in naïve (T<sub>N</sub>, CD45RA<sup>+</sup>/CCR7<sup>+</sup>), central memory (T<sub>CM</sub>, CD45RA<sup>-</sup>/CCR7<sup>+</sup>), effector memory (T<sub>EM</sub>; CD45RA<sup>+</sup>/CCR7<sup>-</sup>), and CD45RA<sup>+</sup> effector memory (TEMRA; CD45RA<sup>+</sup>/CCR7<sup>-</sup>) cells (Rufer et al, 2003; Sallusto et al, 1999). These subsets display distinct differentiation states, tissue-homing properties, and functional profiles. We therefore investigated

whether they also showed differential responsiveness to IFNλ stimulation. Individual CD8<sup>+</sup> T-cell subpopulations were purified, stimulated with 1,000 IU/ml IFNα or 100 ng/ml IFNλ1 and analyzed by Western blotting for activation of STAT1 (pY-STAT1). All populations responded to IFNα stimulation (Fig 4I). In contrast, IFNλ1 induced phosphorylation of STAT1 predominantly in TEMRA cells and only to a lesser extent in the T<sub>CM</sub> cells. T<sub>N</sub> and T<sub>EM</sub> did not show a response to IFNλ1 stimulation. As TEMRA cells mount rapid and robust IFNγ responses (Sallusto et al, 1999) and given their unique sensitivity to IFNλ1, these cells are likely to be the major targets for the IFNγ-boosting properties of IFNλ.

Next, we investigated whether IFNλ could synergize with IFNα in enhancing CD8<sup>+</sup> T-cell responses induced by suboptimal TCR-triggering (Nguyen et al, 2002; Curtsinger et al, 2005; Hervas-Stubbbs et al, 2010). Combinations of IFNα, IFNλ1, and IFNλ4 in the absence or presence of suboptimal doses of anti-CD3 mAbs were therefore used. No synergistic or antagonistic effects of IFNs were observed (Fig 4J). Taken together, these results indicated that IFNλs might amplify CD8<sup>+</sup> T-cell effector functions induced by suboptimal antigenic stimuli, similarly to what has been described for IFNα (Curtsinger et al, 2005). Furthermore, no inhibitory effect of IFNλ4 on IFNγ production induced by IFNα or IFNλ1 was observed.

**Impact of IFNλ4 genotype on intrahepatic T cells in patients with CHC**

To investigate whether there were main differences in T cells between IFNλ4 genotype ΔG and TT patients, immunohistochemical analysis was performed on liver tissue of a cohort of CHC patients. We focused on determining the relative frequencies of PD1<sup>+</sup> T cells in the liver as this marker is expressed on activated T cells and is associated with inhibition of the immune response. Accordingly, we performed CD3/PD1 co-staining on sections of paraffin-embedded liver tissue (Fig 5B and C) obtained from 20 CHC patients of IFNλ4 genotype ΔG and 19 of IFNλ4 genotype TT (Table 1). This analysis revealed that there was no difference in the frequency of CD3<sup>+</sup>/PD1<sup>+</sup> cells in the liver of ΔG and TT CHC patients (Fig 5A–C), thus excluding differential accumulation of T cells and expression of PD1 as reason of virus persistence in IFNλ4-producer patients.

The functional differences between ΔG and TT patients might be associated with more subtle changes in unique populations of T cells. Therefore, we performed a multicolor Flow cytometry analysis

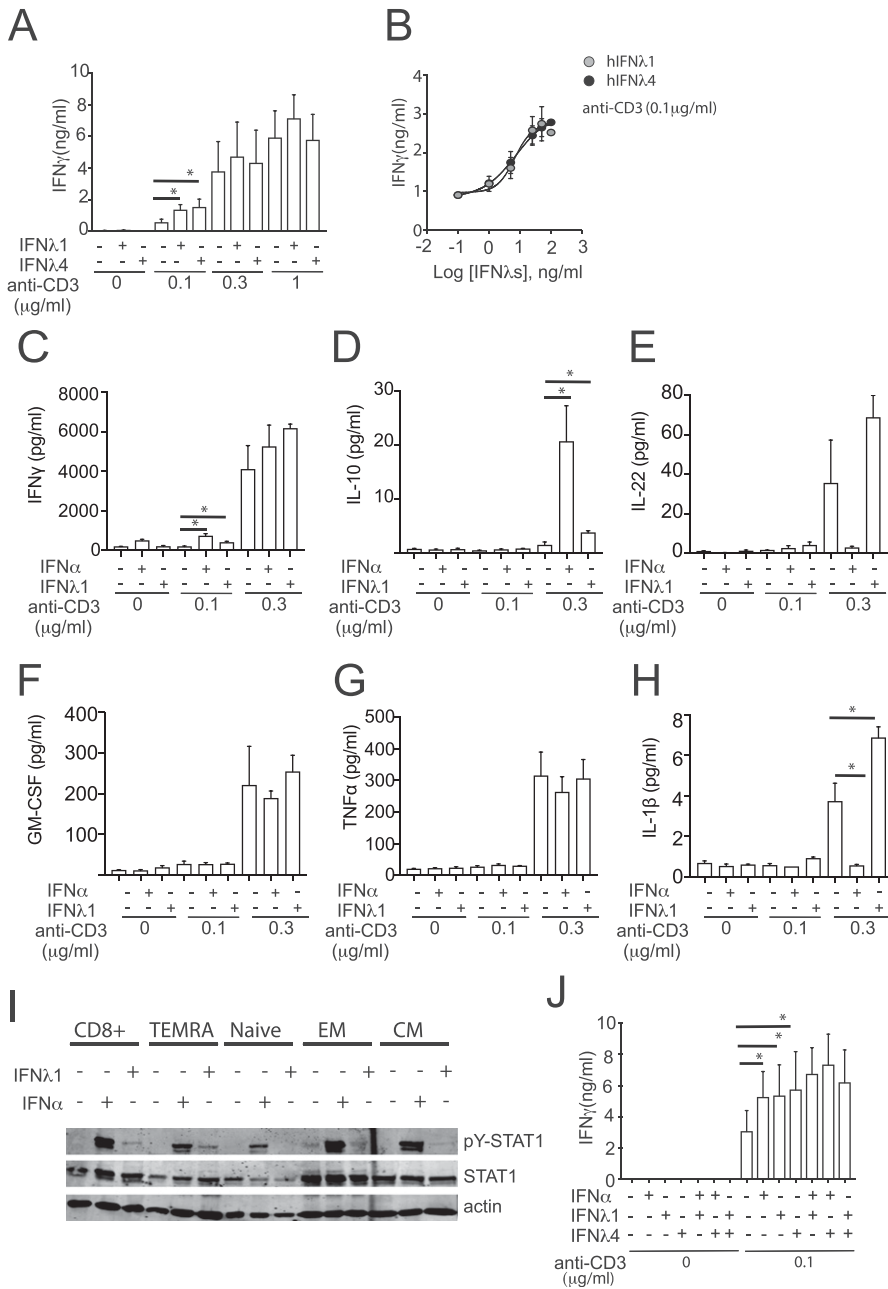


**Figure 4. IFN $\lambda$ 4 provides a co-stimulatory role during CD8<sup>+</sup> T-cell activation.**

(A, B) CD8<sup>+</sup> T cells were plated for 48 h either (A) on a 96-well plate pre-coated with three different concentrations of anti-CD3 (0.1; 0.3 and 1  $\mu$ g/ml) in the presence of IFN $\alpha$  (1,000 IU/ml), IFN $\lambda$ 1 (100 ng/ml), or IFN $\lambda$ 4 (100 ng/ml) or (B) on a 96-well plate pre-coated with 0.1  $\mu$ g/ml of anti-CD3 in the presence of increasing doses of IFN $\lambda$ 1 and IFN $\lambda$ 4. Released IFN $\gamma$  was determined by ELISA. Data are representative of three independent experiments. (C, D, E, F, G, H) CD8<sup>+</sup> T cells were plated for 48 h either on a 96-well plate pre-coated with three different concentrations of anti-CD3 (0.1 and 0.3  $\mu$ g/ml) in the presence of IFN $\alpha$  (1,000 IU/ml) or IFN $\lambda$ 1 (100 ng/ml). (C, D, E, F, G, H) Released IFN $\gamma$  (C), IL-10 (D), IL-22 (E), GM-CSF (F), TNF $\alpha$  (G), and IL-1 $\beta$  (H) were determined using Meso Scale Discovery assay. Data are representative of three independent experiments. (I) Total CD8<sup>+</sup> and purified TEMRA, naive, EM, and CM CD8<sup>+</sup> T-cell populations were stimulated with IFN $\alpha$  (1,000 IU/ml) or IFN $\lambda$ 1 (100 ng/ml) for 15 min. Phosphorylated STAT1 (pY-STAT1), total STAT1, and actin protein were analyzed by Western blotting using total cellular extracts. A representative blot from two independent experiments is shown. (B, J) CD8<sup>+</sup> T cells were treated with individual or combinations of IFN $\alpha$  (1,000 IU/ml), IFN $\lambda$ 1 (100 ng/ml), and IFN $\lambda$ 4 (100 ng/ml) for 48 h in the presence or absence of anti-CD3 mAbs stimulation and analyzed as described in (B). (A, D) Mean  $\pm$  SEM from three independent experiments (n = 3 for A, D) are shown. \**P* < 0.05, \*\**P* < 0.01, and \*\*\**P* < 0.001 (paired *t* test).

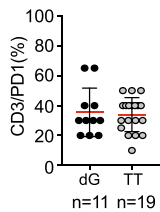
detecting 15 markers in T cells isolated from the liver of nine  $\Delta$ G and four TT CHC patients.

A Wilcoxon test was used to identify differences in the number of cells with a positive phenotype of each surface marker used in the FACS analysis (Fig 6A). These studies showed lack of significant difference in any marker, indicating that there was no enrichment for any one specific population between  $\Delta$ G and TT patient genotypes when individual markers were considered. As PD1 marker was present in this panel, the flow cytometry data confirmed the histological data for this surface protein.

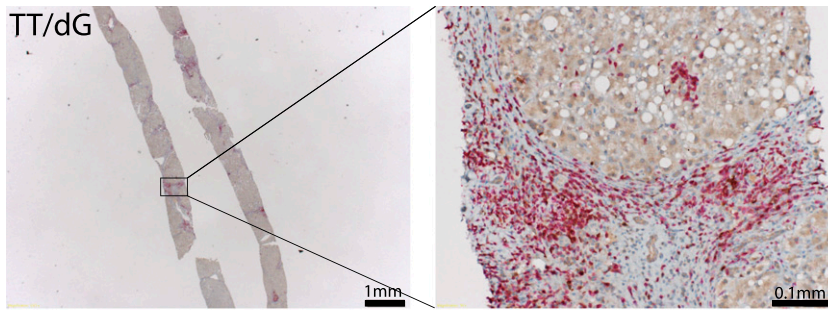
A further analysis was made to determine the presence of unique T-cell populations defined by co-expression of different

markers. A large-data optimized tSNE algorithm, opt-SNE (Belkina et al, 2019 Preprint), was used to embed the high-dimensional FACS data into a low dimensional space amenable to density and phenotype clustering using a combination of DBScan and binary clustering methods (Hahsler & Piekenbrock, 2018; Spagnuolo, 2018). This analysis showed the presence of a large number of clusters, some of which were either represented by a sole patient, or were not enriched in cells from either IFN $\lambda$ 4 producers ( $\Delta$ G) or non-producers (TT) and thus could not reveal any IFN $\lambda$ 4-genotype-dependent phenotypes. To identify phenotypically distinct clusters that were enriched for either the TT or  $\Delta$ G phenotype and representative of all patients with either IFN $\lambda$ 4-genotype, we used a

A



B



C

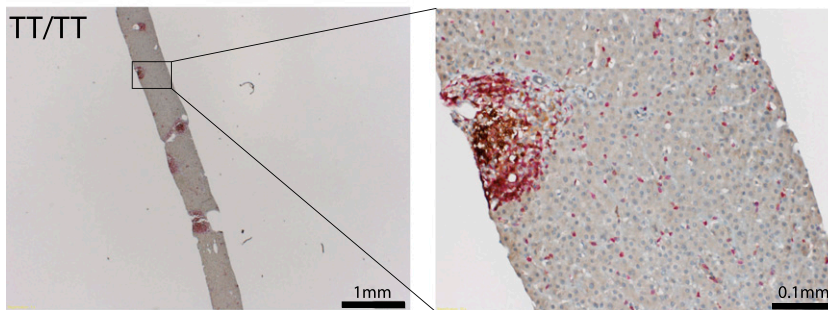


**Figure 5. Detection of CD3<sup>+</sup>/PD1<sup>+</sup> cells in the liver of chronic hepatitis C patients.**

(A) Paraffin-embedded liver biopsies were stained using mAbs specific for CD3 and PD1 (A) Frequency of CD3<sup>+</sup>/PD1<sup>+</sup> cells in the liver of chronic hepatitis C patients with ΔG and TT IFNλ4 genotype. (B, C) Representative bright-field images of CD3 and PD1 staining of liver sections of a patient of TT/ΔG genotype and (C) TT/TT genotype. Red, CD3 signal; brown, PD1 signal.

Poisson ratio test which was additionally controlled for patient equality and diversity using the Gini-coefficient and Gini-Simpson index, respectively (Fig 6B and C). Clusters whose IFNλ4 ΔG/TT genotype ratio was in the top and bottom 10<sup>th</sup> percentile and had a false discovery rate of >0.001 were considered to be significantly enriched. This resulted in 100 phenotypically distinct clusters (Fig 6D) that are broadly clustered by expression of CD8, 2B4, KLRG1, CD127, and CD57 markers.

From these TT and ΔG genotype-enriched clusters, two main groups were immediately apparent with opposing CD57 and CD127 phenotypes. The CD57<sup>+</sup> CD127<sup>-</sup> group was constituted mostly by CD8<sup>+</sup> KLRG1<sup>+</sup> 2B4<sup>+</sup> TT-enriched clusters (Fig 6D annotation 1). Both CD57 and 2B4 markers are indicators of senescence and exhaustion in CD8<sup>+</sup> T cells, respectively (Brenchley et al, 2003; West et al, 2011). Together with the CD45RO<sup>-</sup> CD127<sup>-</sup> and KLRG1<sup>+</sup> phenotypes in this group, these findings indicate that IFNλ4 non-producing patients display larger numbers of T cells with senescent and exhausted phenotypes typical of chronic immune activation in response to viral infection.

In contrast, the CD57<sup>-</sup> CD127<sup>+</sup> group contained two CD8<sup>+</sup> subgroups; CD8<sup>+</sup> CD45RO<sup>-</sup> and CD8<sup>+</sup> CD45RO<sup>+</sup>, both of which had an even split between TT- and ΔG-enriched clusters (Fig 6D annotations 2, 3). The expression of both KLRG1 and 2B4 within these two groups, although not entirely absent, was markedly reduced than

that seen in the CD8<sup>+</sup> CD57<sup>+</sup> group. Taken together, this analysis suggests a preponderance for CD8<sup>+</sup> TT cells to enter a senescent or exhausted phenotype upon repetitive activation.

To further explore the progressive nature of the expression of markers that describe their differentiation states, TT and ΔG cells were ordered according a pseudotime based on the expression of CD57, KLRG1, PD1, and TIM3 markers using a diffusion mapping algorithm (Angerer et al, 2016). Significantly enriched clusters were split into five groups for each IFNλ4-genotype including: total CD8<sup>+</sup>, CD8<sup>+</sup> CD161<sup>+</sup>, CD8<sup>+</sup> CD161<sup>-</sup>, CD4<sup>+</sup>, and CD8<sup>+</sup> CD4<sup>-</sup> (DN) subpopulations. CD161 was chosen as it marks an important population of T cells in the liver with unique transcriptional and functional phenotype (Northfield et al, 2008; Fergusson et al, 2014).

By examining the distribution of cells along the pseudotemporal axis, it was apparent that TT CD8<sup>+</sup> cells were predominantly located at the end of the pseudotemporal ordering in a CD57<sup>+</sup> KLRG1<sup>+</sup> state independently of their CD161 phenotype (Figs 7 and 8). In contrast, total ΔG CD8<sup>+</sup> cells were predominantly distributed at the beginning in a KLRG1<sup>-</sup> CD57<sup>-</sup> CD127<sup>+</sup> state (Figs 7 and 8).

Closer analysis of the CD8<sup>+</sup> population by splitting into CD161<sup>+</sup> and CD161<sup>-</sup> populations revealed exceptions to this general observation. The CD8<sup>+</sup> CD161<sup>-</sup> TT population showed distribution of cells in both early and late pseudotime, whereas the CD8<sup>+</sup> CD161<sup>-</sup> ΔG

**Table 1. Characteristic of patients included in the study.**

Nr	Gender	Age at biopsy	rs815 (IFNL4)	HCV genotype	Log <sub>10</sub> (viral load)	Metavir	FACS	Immunohistochemistry
1	f	64	ΔG/ΔG	1b	5.44	A2/F1	X	X
2	m	58	ΔG/ΔG	3a	5.47	A3/F3	X	X
3	m	24	ΔG/ΔG	1	4.81	A1/F0	X	X
4	m	49	ΔG/ΔG	4	6.50	A1/F1		X
5	m	61	ΔG/ΔG	1b	n.a	A2/F2		X
6	m	51	ΔG/ΔG	1b	5.75	A2/F4		X
7	m	40	ΔG/ΔG	3a	5.66	A1/F1		X
8	f	53	ΔG/ΔG	4a/c/d	5.90	A3/F3		X
9	m	48	ΔG/ΔG	4a/c/d	6.03	A2/F2		X
10	m	30	ΔG/ΔG	1a	5.03	A1/F1		X
11	m	24	ΔG/ΔG	1a	5.26	A1/F0		X
12	m	52	TT/ΔG	3a	6.69	A2/F2	X	X
13	m	56	TT/ΔG	3a	5.75	A3/F4	X	X
14	m	50	TT/ΔG	1a	6.92	A3/F2	X	X
15	f	37	TT/ΔG	1a	n.a	A1/F2	X	X
16	m	46	TT/ΔG	4a/c/d	5.06	A3/F4	X	X
17	m	45	TT/ΔG	1b	5.25	A1/F1	X	X
18	M	15	TT/ΔG	1a	5.44	A1/F1		X
19	f	47	TT/ΔG	1a	6.78	A2/F4		X
20	m	45	TT/ΔG	1a	6.21	A2/F2		X
21	m	42	TT/TT	3a	6.98	A2/F1	X	X
22	f	52	TT/TT	4	n.a	A2/F2	X	X
23	m	77	TT/TT	1b	5.92	A2/F3	X	X
24	m	61	TT/TT	1a	n.a	A2/F1	X	X
25	m	43	TT/TT	1	5.97	A1/F1		X
26	f	45	TT/TT	3a	5.06	A1/F1		X
27	f	45	TT/TT	1b	6.38	A2/F1		X
28	m	53	TT/TT	n.a	6.47	A2/F2		X
29	f	52	TT/TT	1a	6.09	A2/F1		X
30	m	36	TT/TT	3a	5.90	A1/F1		X
31	m	43	TT/TT	1a	3.60	A1/F1		X
32	m	39	TT/TT	3a	6.41	A1/F1		X
33	f	41	TT/TT	1b	6.44	A2/F3		X
34	m	50	TT/TT	3a	6.52	A2/F1		X
35	m	53	TT/TT	3a	6.52	A3/F4		X
36	m	56	TT/TT	1a	6.80	A3/F3		X
37	m	45	TT/TT	3a	5.87	A2/F4		X
38	f	37	TT/TT	1a	6.19	A2/F3		X
39	m	53	TT/TT	4	6.12	A1/F1		X

population was preferentially distributed in early pseudotime (Fig 8). Furthermore, the CD8<sup>+</sup> CD161<sup>-</sup> ΔG population showed decrease in CD127 expression correlating with the increase in expression of CD57, KLRG1, 2B4, and PD1. Taken together, these findings indicated

a limited accumulation of cells with senescent/exhaustion phenotype in ΔG patients.

Important differences were observed also in the CD8<sup>+</sup> CD161<sup>+</sup> populations. Whereas CD8<sup>+</sup> CD161<sup>+</sup> ΔG and TT cells displayed almost



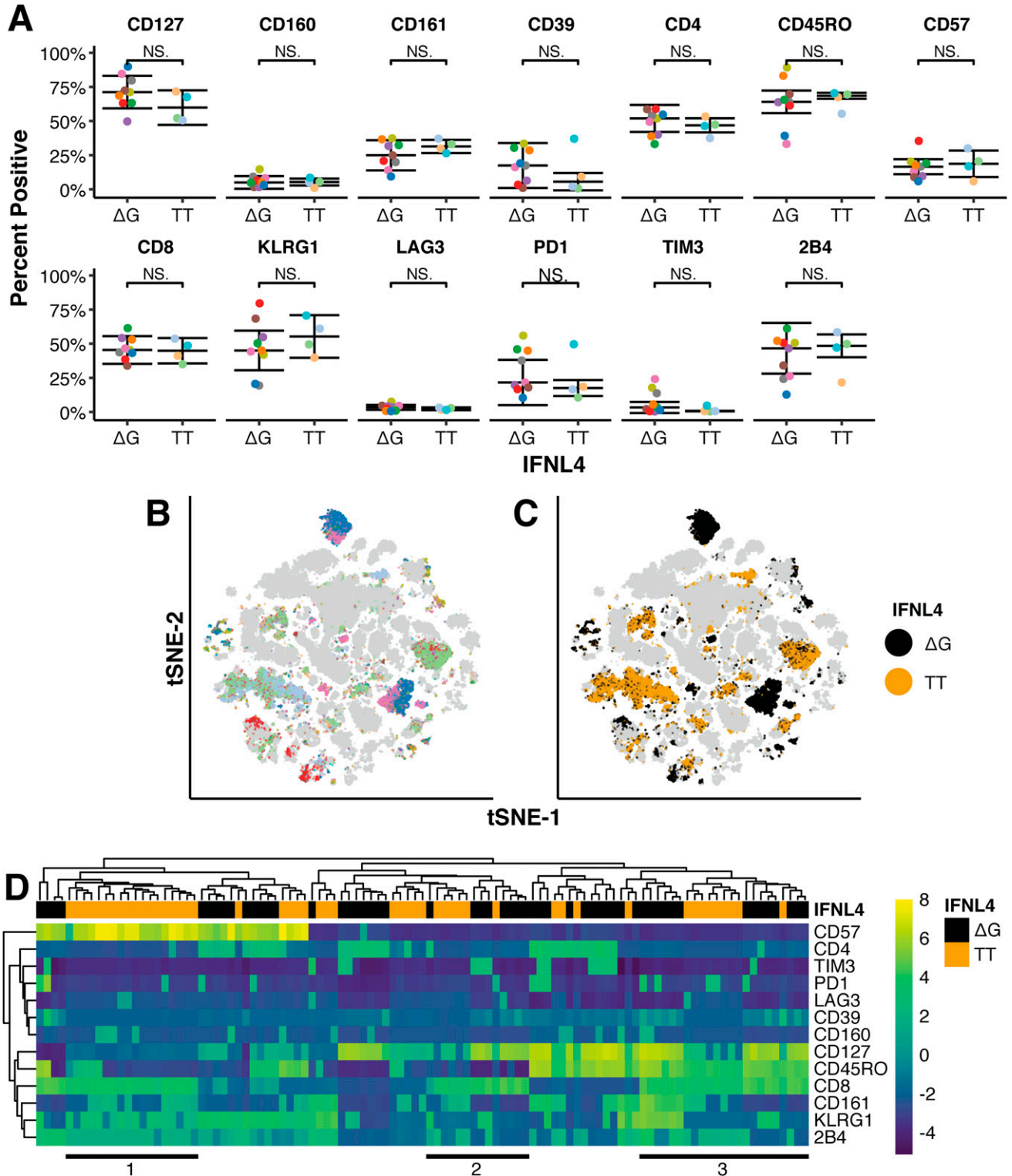


**Figure 6. Phenotypic characterization and multidimensional analysis of patient liver biopsies.** Intrahepatic lymphocytes (IHLs) were isolated from fresh liver biopsy tissue obtained from chronically hepatitis C virus–infected patients either carrying the IFNL4  $\Delta G$  or TT allele. IHLs were subjected to multicolor FACS analysis. **(A)** *t* tests identified no significant differences ( $P > 0.05$ ) in the percent of cells with a positive phenotype for any cell surface marker between patients with  $\Delta G$  ( $n = 9$ ) or TT ( $n = 4$ ) IFNL4 alleles. **(B, C)** tSNE dimensional reduction and clustering enabled identification of clusters enriched for either IFNL4 allele (C) using a Poisson test (false discovery rate  $< 0.001$ ; colored dots) while maintaining within-cluster representation of patients with each IFNL4 allele (B). Cells not selected for further analysis are gray. **(B, C, D)** Hierarchical clustering of the median marker expression of selected clusters from (B) and (C), revealing three groups (1, 2, 3) of CD8<sup>+</sup> clusters with opposing expression of exhaustion and senescence markers CD57, CD127, KLRG1, PD1, and 2B4.

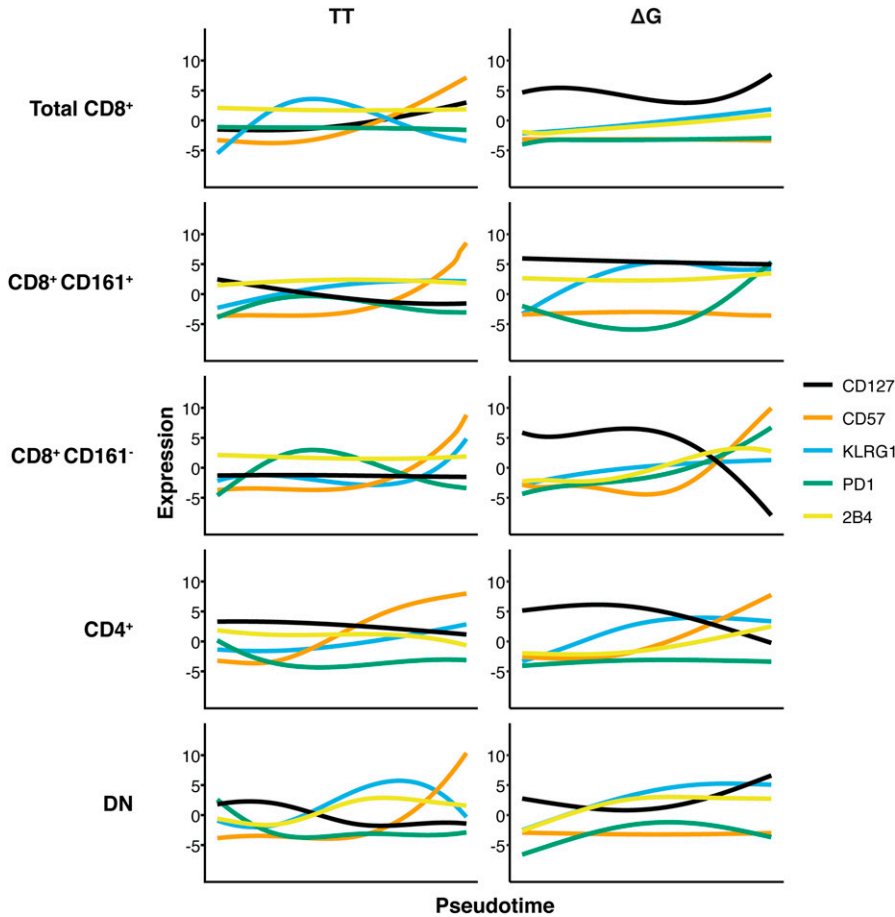


**Figure 7. Pseudotime ordering of CD8<sup>+</sup>, CD4<sup>+</sup>, and double-negative cell populations indicates differentiation state-dependent changes in exhaustion and senescence markers.** IFNλ4 allele enriched clusters were embedded by diffusion mapping and temporally ordered based on the co-expression of CD57, KLRG1, PD1, and TIM3. Curves fitted to the temporally ordered cells indicate smoothed average of marker expression.

similar temporal distribution (Fig 8), in TT cells, expression of CD127 negatively correlated to the expression of CD57 and KLRG1 (Pearson = -0.66 and -0.50, respectively). That is, these cells are CD127-highly positive at the beginning of the temporal ordering and become CD127-negative as expression of KLRG1 and CD57 increases. In contrast, the CD8<sup>+</sup> CD161<sup>+</sup> ΔG cells did not show a pseudotime-dependent relationship between the expression of CD127, CD57, and KLRG1; showing no pseudotime-dependent change in CD127 or CD57 phenotypes across the temporal axis, which remained high and low, respectively. Nevertheless, this population did show a pseudotime-dependent increase in the expression of KLRG1 and PD1. These findings indicated that in CD8<sup>+</sup> CD161<sup>+</sup> ΔG cells, there were fewer cells expressing the exhaustion-associated marker CD57 and more cells expressing the PD1 and CD127 markers, indicating previous cell activation (Larbi & Fulop, 2014).

The analysis also showed that there were no major differences between CD4<sup>+</sup> TT and CD4<sup>+</sup> ΔG populations, which mostly distributed early in pseudotime and displayed expression patterns similar to that of the CD8<sup>+</sup> CD161<sup>+</sup> ΔG cells.

CD4<sup>-</sup> CD8<sup>-</sup> DN TT and ΔG cells were temporally distributed towards the end of the continuum, similarly to the distribution of CD8<sup>+</sup> CD161<sup>+</sup> TT and ΔG cells. However, only the double-negative TT cells displayed a pseudotime-dependent increase in CD57 and KLRG1 expression correlating with a decrease in CD127 expression. The DN ΔG cells remained CD127<sup>+</sup> without any change in CD57, despite an increase in KLRG1 over time.

In conclusion, such analysis showed that only CD8 and DN cells differed between IFNλ4-producer (ΔG) and non-producer (TT) patients. In particular, in TT patients the CD8<sup>+</sup> 161<sup>-</sup> population showed a phenotype of cells with senescent phenotype, which might reflect repetitive activation during chronic infection. On the contrary, in ΔG patients the same population showed marked tendency to remain partially activated and without evidence of senescence/exhaustion.

## Discussion

HCV infection triggers a rapid and strong innate immune response characterized by induction of a large variety of ISGs (Heim & Thimme, 2014). Despite activation of this important arm of innate immunity, clearance of acute HCV infection depends on activation of virus-specific CD4 and CD8 T cells (Grakoui et al, 2003; Shoukry et al, 2003). HCV clearance is also facilitated by a genetic polymorphism that prevents production of active IFNλ4. Indeed, the wild-type allele of *IFNL4* gene that encodes a functional IFNλ4 protein is associated with inefficient adaptive immune responses and development of chronic HCV infection (Terczynska-Dyla et al, 2014). The link between *IFNL4* genotypes and the cellular immune response against HCV remains to be determined. As the IFNLR was found mostly expressed by epithelial cells (Sommereyns et al,

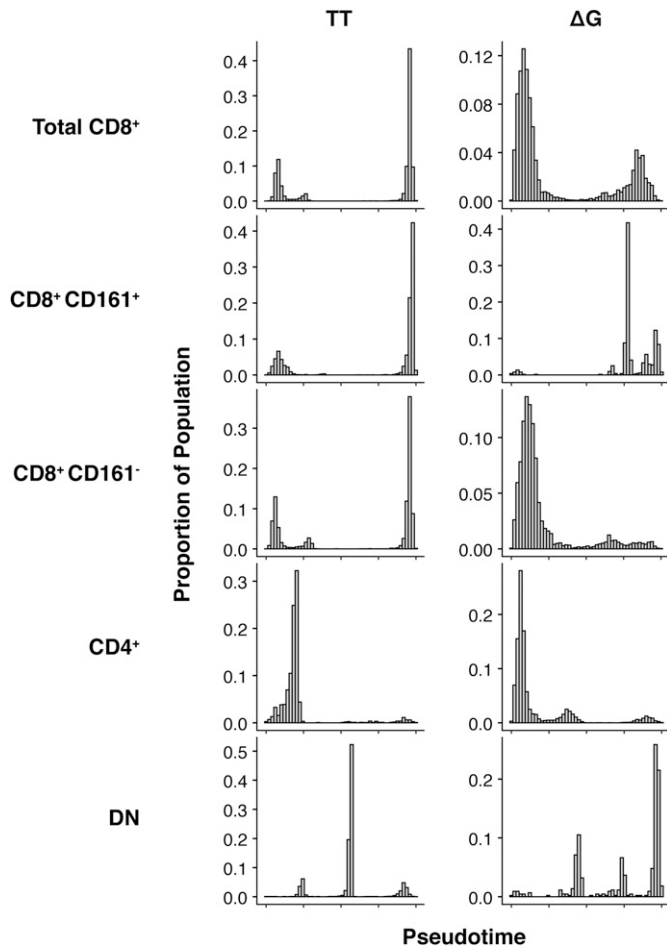


**Figure 8. Distribution of cells across pseudotime.**

The proportion of cells is differentially distributed across pseudotime in a lineage-dependent manner. Total CD8<sup>+</sup> TT cells (n = 14,081) are distributed late in the temporal ordering, whereas total CD8<sup>+</sup> ΔG cells (n = 6,230) are distributed earlier. No difference was observed in the temporal distribution of CD8<sup>+</sup> CD161<sup>+</sup> TT or ΔG cells (n = 4,226 and 513, respectively). In contrast, an IFNλ4-dependent differential distribution of cells was observed in CD8<sup>+</sup> CD161<sup>+</sup> TT and ΔG cells (n = 9,855 and 5,717, respectively). CD4<sup>+</sup> TT and ΔG cells (n = 1,591 and 6,959, respectively) were temporally distributed similarly to CD8<sup>+</sup> TT cells. Double-negative (DN) TT and ΔG cells (n = 6,722 and 437, respectively) were distributed similarly to CD8<sup>+</sup> CD161<sup>+</sup> cells.

2008), it remains also unclear whether IFNλ regulate immune response in a direct or indirect manner. Several immunomodulatory activities of IFNλ1-3 have been described, including the up-regulation of IL-6, IL-8, and IL-10 production in PBMCs (Jordan et al, 2007a), alteration of the Th1/Th2 T-cell balance (Jordan et al, 2007b), reduction of IL-13 production by T cells (Srinivas et al, 2008), or induction of ISGs in B cells (de Groen et al, 2015) and in plasmacytoid dendritic cells (Kelly et al, 2016). It remains unclear whether also IFNλ4 has immunomodulatory capacities (Heim et al, 2016).

In the present study, we investigated whether different IFNλs affect B- and T-cell functions, and in particular whether IFNλ4 has immunosuppressive functions, which could support its inhibitory role in the adaptive host response to HCV infection. Using STAT1 activation as readout for IFNλ stimulation, we directly assessed cell activation through IFNLR triggering. We found that only B and CD8

T cells, isolated from circulating blood of healthy donors, respond to IFNλ. The strongest STAT1 phosphorylation was detected in B cells and the strength of STAT1 activation in different lymphocytic populations correlated with the *IFNLR1* transcripts. These findings are consistent with other studies reporting that B cells express the highest levels of *IFNLR1* mRNA among PBMCs (Witte et al, 2009). In addition, and consistent with a previous report (Rivera, 2019), we found neutrophils to be responsive to IFNλ.

Further characterization of the IFNλ-responsive B-cell populations revealed that both CD27-negative cells (enriched in naïve populations) and CD27-positive cells (enriched in memory B cells) responded to IFNλ. In contrast, among CD8<sup>+</sup> T cells, effector memory cells (TEMRA) were the most responsive followed by central memory cells, whereas naïve cells were nonresponsive. CD4 T-cell populations instead did not show STAT1 phosphorylation upon incubation with IFNλ. Monocytes did not respond to IFNλ probably caused by a very low expression of the *IFNLR1*, as previously reported (Mennechet & Uze, 2006; Liu et al, 2011). When CD14 monocytes were differentiated into dendritic cells, they acquired IFNλ responsiveness, as previously reported (Mennechet & Uze, 2006).

Having identified the lymphocyte populations reacting to IFNλ, we studied several possible immunosuppressive effects. We detected no differences of JAK-STAT signaling in B cells and CD8 T cells after stimulation by IFNλ1 and IFNλ4, thus suggesting that IFNλ4 acts as a *bonafide* IFN in this regard, similarly to other type I IFNs. IFNλ4 also did not interfere with the other IFNs using different activation assays. IFNλ exerted minimal direct effects on B-cell activation as measured by changes in CD69 expression levels, despite expression of *IFNLR1*. It also showed synergistic effects with TLR9 stimulation of B cells, although with lower efficacy than other type I IFNs.

In another series of experiments, we studied whether IFNλ4 interferes with antibody production by B cells. Most of HCV-infected patients produce antibodies against structural and non-structural HCV proteins during the acute phase of infection (Logvinoff et al, 2004). Whether these antibodies participate in HCV clearance remains unclear. We did not find inhibitory activity of IFNλ4 on TLR9 induced IgG production, confirming that IFNλ4 is similar to other tested IFNs also in this regard.

Like other IFNs, IFNλ4 increased the release of the immunosuppressive IL-10 cytokine, when B cells were co-stimulated with TLR9 ligand. However, even larger increased IL-10 production was induced by IFNα and IFNλ1, thus excluding that this mechanism is unique to IFNλ4.

Both IFNλ1 and IFNλ4 promoted the release of IFNγ by T cells upon suboptimal stimulation with anti-CD3 monoclonal antibodies. Similarly, IFNλ stimulation promoted the secretion of anti-inflammatory cytokines IL-10 and IL-22. Surprisingly, stimulation in the presence of IFNλ4 and IFNα exerted different effects on secretion of IL-1β, with a significant increase of this pro-inflammatory cytokine observed only with IFNλ. Although it is known that type I IFNs have anti-inflammatory properties because they inhibit IL-1β secretion (Huang et al, 1995; Billiau, 2006), little is known on the effects of type III IFN on IL-1β secretion. One study reported that IFNλ drives a pro-inflammatory phenotype during monocytes differentiation, increasing the secretion of inflammatory mediators including CCL2, IL-1β, and TNF (Read et al, 2019). IL-1β promotes inflammation by inducing the expression of proinflammatory genes, by recruiting immune cells to the site of

infection, and by modulating infiltrating cellular immune-effector action. Interestingly, CHC patients exhibited elevated levels of serum IL-1 $\beta$  compared with healthy controls (Negash et al, 2013). Further studies are required to understand the mechanism of IFN $\lambda$  regulation of IL-1 $\beta$  secretion.

The most responsive populations were TEMRA and CM CD8 T cells, whereas naïve CD8 T cells were non-responsive. These findings were in accordance with the STAT1 phosphorylation studies and with detected up-regulation of IFNR genes, but do not explain the immunosuppressive effects of IFN $\lambda$ 4. They indicate that type I IFNs sustain the effector functions of primed and antigen-responding CD8 T cells, whereas they probably have minor effects during T-cell priming with antigen.

Another reported effect of stimulation with IFN $\alpha$  is induction of inhibitory receptors in T cells (Francisco et al, 2010; Terawaki et al, 2011). Therefore, we attempted to correlate the presence of CD3<sup>+</sup>PD1<sup>+</sup> cells in the liver of HCV patients with IFN $\lambda$ 4-producer and non-producer genotype. These immunohistochemistry studies revealed the presence of PD1-expressing T cells, whose numbers, however, were not significantly different in the two groups of patients.

Significant differences were instead observed using multicolor flow cytometry. Using tSNE analysis we identified several clusters of T-cell populations. These clusters were further selected for their representation in all patients and classified for enrichment in either TT or  $\Delta$ G donors. Major differences were detected in the CD8 and DN populations, but not in CD4 cells, indicating alterations only in cell populations which reacted to IFN $\lambda$ 4 in vitro. When cells were distributed using a pseudotime order, together with expression of the CD161 marker, cells from TT or  $\Delta$ G donors differed in multiple ways. Indeed, CD8<sup>+</sup>CD161<sup>-</sup>  $\Delta$ G cells showed preferential distribution in the early phase of pseudotime and did not express the PD1, KLRG1, 2B4, and CD57 markers. Instead, they showed high expression of CD127, a marker mostly expressed by central memory T cells and positively correlating with expression of CD28 (Larbi & Fulop, 2014). As CD127 participates in the regulation of host cell homeostasis, proliferation of differentiated T cells, and also in cell survival, these cells might represent a potentially still active population without evidence of senescence or exhaustion (Larbi & Fulop, 2014). On the contrary, the minor population of CD8<sup>+</sup>CD161<sup>-</sup>  $\Delta$ G cells distributing in the late pseudotime dimension resembled the corresponding population from TT donors. These T cells expressed high levels of PD1, KLRG1, 2B4, and CD57, thus resembling senescent/exhausted cells. The reason of the accumulation in IFN $\lambda$ 4-producers of CD8 T cells with central memory-like and not senescent phenotype is intriguing. It is tempting to speculate that as the affected T-cell populations are the same showing direct response to IFN $\lambda$ 4 in vitro, the effect is T-cell intrinsic. As CD8<sup>+</sup>CD161<sup>-</sup> cells belong to the classical population of adaptive T cells, these cells might become low responders to the antigen, thus proliferating slowly in the presence of IFN $\lambda$ 4. This effect could be obtained by direct interference of IFNLR signaling with antigen responsiveness. Indeed, during LCMV infection in mice, STAT1 activation in T cells induced inhibition of CD8 cell proliferation (Gil et al, 2006). Future studies will address the molecular mechanisms of IFN $\lambda$ 4 on CD8<sup>+</sup>CD161<sup>-</sup> cells.

The second affected population was represented by CD8 cells expressing CD161. These cells are abundant in the liver and in other

mucosal tissues. They frequently recognize non-MHC-restricted antigens, express chemokine receptors associated with tissue homing in resting and inflammatory conditions (Billerbeck et al, 2010), and proliferate in the presence of IL-12 and IL-18 independently of TCR stimulation (Ussher et al, 2014). These cells were found mostly in the late pseudotime and only in  $\Delta$ G donors. They showed high expression of PD1, KLRG1, CD127, and lack of CD57. These cells therefore represent a population which is not exhausted, although it expresses typical markers of TEMRA cells (Larbi & Fulop, 2014). As for the CD8<sup>+</sup>CD161<sup>-</sup> cells, also in this case, it remains unknown the molecular mechanism leading to the accumulation in  $\Delta$ G donors of cells with these unique phenotypes. As speculated with CD8<sup>+</sup>CD161<sup>-</sup> cells, it could be that IFN $\lambda$ 4 reduces antigen responsiveness, thus limiting CD57 expression, and without limiting antigen-independent proliferation after stimulation with IL-12 and IL-18. Indeed, expression of CD57 has been associated with persistent antigenic stimulation and critically shortened telomeres (Brenchley et al, 2003) and does not occur after proliferation induced by IL-12 or IL-18 (Kurioka et al, 2018).

In contrast with other reports (Srinivas et al, 2008), our data demonstrate that CD4 cells do not respond to IFN $\lambda$  probably because of low IFNLR expression according to our PCR data. Although CD4 cells are not responsive to IFN $\lambda$  stimulation, they could be indirectly modulated by IFN $\lambda$ 4 through its effects on B and CD8 T cells, or dendritic cells. Clarification of these possibilities would require detailed analysis of intrahepatic lymphocytes isolated from a large cohort of CHC patients because IFN $\lambda$ 4 gene is not expressed in mice (Wack et al, 2015).

In conclusion, our results show that IFN $\lambda$ 4 displays typical IFN activities and acts directly on unique populations of immune cells. The same populations of T cells are affected in the liver of IFN $\lambda$ 4-producer donors indicating T-cell-intrinsic effects, which lead to limited senescence after antigen stimulation.

## Materials and Methods

### Healthy blood donors

Blood samples were obtained from Regional Blood Transfusion Service, Swiss Red Cross, Basel, from healthy male and female donors (18–65 yr old) as buffy coats. All donors gave written informed consent.

### Human liver biopsies and DNA isolation

Liver biopsies and blood samples (EDTA-anticoagulated blood) were obtained from HCV-infected patients (n = 13) (patients characteristics are shown in Table 1) in the outpatient clinic of the Division of Gastroenterology and Hepatology, University Hospital Basel, Switzerland. Biopsy material that was not needed for routine histopathology was used for research purposes after obtaining written informed consent. The use of biopsy material for this project was approved by the Ethikkommission Nordwest- und Zentralschweiz, Basel, Switzerland, protocol number M989/99. Total DNA was isolated from blood using DNeasy Blood & Tissue Kit (QIAGEN) according to the manufacturer's instructions. IFN- $\lambda$ 4 genotype was determined as described previously (Terczynska-Dyla et al, 2014).

### Isolation and stimulation of PBMCs and liver infiltrating lymphocytes

PBMCs were isolated from blood samples by standard density-gradient centrifugation protocols (SEcoll Human; Seraglob), washed twice in PBS, and analyzed immediately or cryopreserved in freezing medium (90% fetal bovine serum and 10% dimethyl sulfoxide). PBMCs were stimulated with 100 ng/ml IFN $\lambda$ 1 and as control with 1,000 IU/ml IFN $\alpha$ . Total cellular proteins were isolated after 15 min of IFN stimulation and the degree of STAT1 phosphorylation (pY-STAT1) was determined by Western blotting. Liver biopsy samples were collected in PBS and then washed twice again with PBS to remove cell debris and red blood cells. Isolation of liver-infiltrating lymphocytes was performed by mechanical disruption of the tissue through a 40- $\mu$ m cell strainer (Falcon) using a 5-ml syringe plunger (CODAN Medical ApS). The mesh was rinsed twice with PBS to ensure maximal recovery. Infiltrated liver immune cells were cryopreserved in freezing medium.

### Antibodies and reagents

Antibodies, chemicals, and kits are described in Table S1.

### Isolation of cell subpopulations from PBMCs

PBMCs were isolated as described in the previous section. Monocytes, CD3<sup>+</sup>, CD8<sup>+</sup> T, CD4<sup>+</sup> T, and B cells were enriched by positive selection (>90% purity) using magnetic beads, according to the manufacturer's instructions (Miltenyi Biotec). Cells were rested for 2 h in complete medium (RPMI-1640, 10% fetal bovine serum, 50 U/ml penicillin and 50  $\mu$ g/ml streptomycin). Mo-DCs were differentiated in vitro from purified CD14<sup>+</sup> monocytes in the presence of 800 U/ml GM-CSF and 500 U/ml IL-4 as described previously (Nair et al, 2012). CD16<sup>+</sup>/CD3<sup>-</sup> NK cells were isolated from PBMCs stained with anti-CD3 and anti-CD16 antibodies by FACSS. Cell sorting was performed with a BD influx cell sorter (BD Bioscience). For sorting of naïve, TEMRA, EM, and CM CD8<sup>+</sup> T cells, CD8<sup>+</sup> T cells were stained with anti-CCR7 and anti-CD45RA (BD Bioscience) monoclonal antibodies (mAbs). Naïve, EMRA, EM, and CM CD8<sup>+</sup> T cells were identified as CD45<sup>+</sup>/CCR7<sup>-</sup>, CD45<sup>+</sup>/CCR7<sup>+</sup>, CD45<sup>-</sup>/CCR7<sup>-</sup>, and CD45<sup>-</sup>/CCR7<sup>+</sup>, respectively. Cells were rested in complete medium for 2–4 h at 37°C before experimentation. Naïve (CD19<sup>+</sup>/CD27<sup>-</sup>) and memory (CD19<sup>+</sup>/CD27<sup>+</sup>) B cells were isolated from CD19<sup>+</sup> B cells using CD27-capturing beads according to the manufacturer's instructions (Miltenyi Biotec).

### Isolation of neutrophils and migration assay

Neutrophils were isolated from blood samples over a 62.5% Percoll gradient (GE Healthcare) in Ca<sup>2+</sup>- and Mg<sup>2+</sup>-free HBSS as previously described (Mocsai et al, 2000) with a purity of more than 90%.  $5 \times 10^5$  neutrophils were placed into a 24-well PET Transwell (8  $\mu$ m pore membrane). As positive control of 100 nM N-formylmethionine-leucyl-phenylalanine (fMLP; Sigma-Aldrich) was added to the medium placed on the bottom of the wells. IFN $\lambda$ 1 or IFN $\lambda$ 4 were used as stimulus alone or in combination with fMLP. Neutrophils were allowed to migrate for 4 h. After 4 h, the medium was collected, and

migrated neutrophils were counted using FACS. Data are reported of percentage of migrated neutrophils over the total number of neutrophils.

### Total RNA extraction and quantitative PCR

Total RNA from PBMCs was isolated using NucleoSpin RNA (Macherey-Nagel AG) according to the manufacturer's instructions. cDNA was synthesized from 400 ng of total RNA using MultiScribe<sup>TM</sup> Reverse Transcriptase (Applied Biosystems<sup>TM</sup>) and random hexamer primers in a 25- $\mu$ l reaction. For all samples, “-RT” controls (reactions omitting the reverse transcriptase) were performed. Real-time qRT-PCR was performed using FastStart Universal SYBR Green Master (Roche Diagnostics AG) or TaqMan Universal PCR Master Mix No AmpErase UNG (Thermo Fischer Scientific) using an ABI 7500 detection system (Applied Biosystems, Thermo Fisher Scientific). Primers and probes are listed in Table S2. The specificity of the PCR products was assessed on a 3% agarose gel and sequenced. Gene transcript expression levels were calculated using the  $\Delta\Delta$ CT method relative to *GAPDH*.

### Whole-cell lysates and immunoblots

Whole-cell lysates and immunoblots were prepared and performed as described previously (Duong et al, 2004) using the following antibodies: Phospho-STAT1 (Tyr701) and  $\beta$ -actin and STAT1 (N-term).

### T-cell activation and cytokines measurement

Human CD8<sup>+</sup> T cells were activated with plate bound anti-CD3 (OKT3; BioLegend) mAbs. 96-well flat bottom plates were coated with anti-CD3 mAbs at different concentrations (1  $\mu$ g/ml; 0.5 and 0.25  $\mu$ g/ml) and incubated overnight at 4°C. Then the coating solution was removed and CD8<sup>+</sup> T cells were added at  $3 \times 10^5$  cells/well. 48 h after activation, cell supernatants were harvested and IFN- $\gamma$  was measured using an IFN- $\gamma$  ELISA. For IFN- $\gamma$  measurement, 96-well plates were coated with 2.5  $\mu$ g/ml of anti-IFN $\gamma$  (BioLegend) antibody and incubated overnight at 4°C. The coating solution was removed and supernatant from activated B cells was added and incubated 2 h at room temperature. Biotin anti-IFN $\gamma$  antibody (1  $\mu$ g/ml) together with HRP Streptavidin (dilution 1/2,000) was used for IFN $\gamma$  detection.

In addition, supernatant was used to measure the secretion of IFN- $\gamma$ , IL-22, IL-10, IL-1B, TNF $\alpha$ , and GM-CSF using U-PLEX Human 4 and 7 plex Biomarker Group 1 (Meso Scale Discovery) following the manufacturer's instructions.

### B-cell activation

CD19<sup>+</sup> cells were stimulated with 1,000 IU/ml IFN $\alpha$  or 100 ng/ml IFN- $\lambda$ 1 or IFN $\lambda$ 4 (kindly provide by Prof R Hartmann) alone or combined with CpG ODN2006 at 0.8 or 2.5  $\mu$ g/ml for 48 h. Cellular activation and surface marker expression was measured by FACS. IgG and IL-10 protein production in the culture supernatants was assessed by ELISA. IgG was measured in the supernatants using sandwich ELISA kits specific for total IgG (detection limit of 1.6 ng/ml) following the manufacturer's (Thermo Fisher Scientific) instructions. For IL-10 measurement, 96-well plates were coated with 2.5  $\mu$ g/ml of anti-

IL-10 (BioLegend) antibody and incubated overnight at 4°C. The coating solution was removed and supernatants from activated B cells were added and incubated for 2 h at room temperature. Biotinylated anti-IL-10 antibodies (1 µg/ml) and HRP-Streptavidin (dilution 1/2,000) were used for IL-10 detection.

### Flow cytometry

PBMCs were subjected to surface staining to identify lymphocyte populations using the mAbs listed in Table S1. Cells were resuspended in staining buffer (PBS containing 0.02% Na<sub>2</sub>S<sub>2</sub>O<sub>8</sub> and 0.5% human albumin) and stained for 20 min at 4°C in the dark. Data were acquired using a BD Accuri C6 (BD Bioscience) or CytoFLEX (Beckman) flow cytometer and analyzed with FlowJo 10.1.r1 (Tree Star). For intracellular staining, cells were fixed and permeabilized with Perm Buffer (BD Bioscience) for 20 min on ice. After washing, cells were incubated with blocking solution (5% BSA in PBS) for 1 h at room temperature. After removal of the blocking solution, cells were incubated with pY-STAT1 antibody or rabbit IgG as control at 4°C overnight. Next day cells were washed and incubated with AlexaFluor 647-labeled goat antirabbit Ig for 1 h at room temperature. After washing, cells were resuspended in PBS and analyzed using BD Accuri C6 (BD Bioscience). Data were analyzed with FlowJo 10.1.r1 (Tree Star).

### Lymphocyte phenotype analysis

Paired intrahepatic lymphocytes and PBMCs were thawed in PBS with 1% DNase to prevent cell clumping. After centrifugation, the cells were resuspended in complete medium and rested for 1 h at 37°C before staining. Cells were washed with PBS/1% DNase and resuspended in blocking buffer (PBS containing 50% human serum) for 30 min at room temperature. For staining, the cells were resuspended in staining buffer (PBS containing 0.02% Na<sub>2</sub>S<sub>2</sub>O<sub>8</sub> and 0.5% human albumin) and antibodies were added for 20 min at 4°C in the dark. After washing, the cells were resuspended on PBS and analyzed using an LSR Fortessa flow cytometer (BD Bioscience). Data were analyzed using FlowJo v10.r1 (Tree Star). CD3<sup>+</sup> living cells were gated and FACS data were exported from FlowJo v10.r1 into the R statistical computing environment and transformed with an inverse hyperbolic sine function (asinh). For further analysis, the transformed data were separated into IHL and PBMC T-cell sets. Each group was subjected to two-dimensional tSNE reduction using the R package *fftRtsne* version 1.0.1 based on the tSNE implementation described by [Linderman et al \(2019\)](#). IFNλ4 genotype specific T-cell clusters were identified by density based spatial clustering using the DBScan ([Hahsler & Piekenbrock, 2018](#)) package version 1.1-3 and the results were plotted using the *ggplot2* package. Clusters containing significantly higher ratios of either IFNλ4 allele were identified by performing Poisson tests using generalized linear mixed effect models (*lme4* [[Bates et al, 2015](#)] package version 1.1-21) with patient IDs as the random variable to account for variability in the total number of cells acquired in each patient. CD4<sup>+</sup>, CD8<sup>+</sup>, and double-negative (CD4<sup>-</sup>CD8<sup>-</sup>) IFNλ4 TT/ΔG-enriched clusters with false discovery rate < 0.05 were split into groups by their CD161 phenotype before pseudotime analysis using *destiny* ([Angerer et al, 2016](#)) version 2.12.0, and expression of CD57, PD1,

KLRG1, and TIM3 markers were used for pseudotemporal ordering. Finally, curves for pseudotemporally ordered marker expression were fitted using *mgcv* ([Wood, 2011](#)) version 1.8-28.

### CD3 and PD1 immunohistochemistry

Immunohistochemical (IHC) staining for CD3 and PD1 was performed on 4-µm sections of formalin-fixed paraffin-embedded liver biopsy tissue obtained from CHC patients. Immunohistochemical staining was performed on a Benchmark immunohistochemistry staining system (Ventana Medical Systems) using primary anti-CD3 and PD1 antibodies (Roche Diagnostic, Table S1) and the iVIEW-DAB chromogenic system for signal visualization as previously described ([Piscuoglio et al, 2012](#)). Specifically, sections were pre-treated with CC1 (Ventana Medical Systems) before incubation with the primary anti-CD3 and PD1 antibodies. The staining signal was then revealed using the iVIEW-DAB system. Negative controls omitting the primary antibody were included in each run. Blind scoring of the immunoreactivity was performed independently by an experienced pathologist (LM Terracciano) and two observers (D Calabrese and M Coto-Llerena).

### Statistical analysis

Data are presented as mean value ± SEM. The data were analyzed with Prism4 (GraphPad Software Inc) using a ratio *t* test. In all analyses, a two-tailed *P* < 0.05 (95% confidence interval) was considered statistically significant. All authors had access to the study data and reviewed and approved the final manuscript.

## Supplementary Information

Supplementary Information is available at <https://doi.org/10.26508/lsa.201900612>.

## Acknowledgements

We thank Hans Henrik Gad and Rune Hartmann for providing recombinant human IFNλ4. We thank Stefan Wieland for scientific assistance and critical revision of the manuscript. Grant support: The work was supported by grants SNF 310030\_166202 to MH Heim, and SNF 310030-173240, KFS-3730-08-2015, and PMB-02-17 to G De Libero.

### Author Contributions

M Coto-Llerena: conceptualization, data curation, formal analysis, validation, investigation, methodology, and writing—original draft. M Lepore: conceptualization, data curation, formal analysis, validation, investigation, visualization, and methodology. J Spagnuolo: data curation and formal analysis. D Di Blasi: investigation and methodology. D Calabrese: investigation and methodology. A Suslov: investigation and methodology. G Bantug: conceptualization. FHT Duong: investigation and methodology.

LM Terracciano: investigation and methodology.  
 G De Libero: conceptualization, formal analysis, supervision,  
 funding acquisition, validation, and writing—review and editing.  
 MH Heim: conceptualization, supervision, funding acquisition,  
 validation, project administration, and writing—review and editing.

### Conflict of Interest Statement

The authors declare that they have no conflict of interest.

## References

- Angerer P, Haghverdi L, Buttner M, Theis FJ, Marr C, Buettner F (2016) destiny: Diffusion maps for large-scale single-cell data in R. *Bioinformatics* 32: 1241–1243. doi:[10.1093/bioinformatics/btv715](https://doi.org/10.1093/bioinformatics/btv715)
- Banko Z, Pozsgay J, Szili D, Toth M, Gati T, Nagy G, Rojkovich B, Sarmay G (2017) Induction and differentiation of IL-10-producing regulatory B cells from healthy blood donors and rheumatoid arthritis patients. *J Immunol* 198: 1512–1520. doi:[10.4049/jimmunol.1600218](https://doi.org/10.4049/jimmunol.1600218)
- Bates D, Machler M, Bolker BM, Walker SC (2015) Fitting linear mixed-effects models using lme4. *J Stat Softw* 67: 1–48. doi:[10.18637/jss.v067.i01](https://doi.org/10.18637/jss.v067.i01)
- Bekeredjian-Ding IB, Wagner M, Hornung V, Giese T, Schnurr M, Endres S, Hartmann G (2005) Plasmacytoid dendritic cells control TLR7 sensitivity of naive B cells via type I IFN. *J Immunol* 174: 4043–4050. doi:[10.4049/jimmunol.174.7.4043](https://doi.org/10.4049/jimmunol.174.7.4043)
- Belkina AC, Ciccolella CO, Anno R, Halpert R, Spidlen J, Snyder-Cappione JE (2019) Automated optimized parameters for t-distributed stochastic neighbor embedding improve visualization and allow analysis of large datasets. *BioRxiv*: 451690. doi:[10.1101/451690](https://doi.org/10.1101/451690) (Preprint posted May 17, 2019).
- Bernasconi NL, Onai N, Lanzavecchia A (2003) A role for Toll-like receptors in acquired immunity: Up-regulation of TLR9 by BCR triggering in naive B cells and constitutive expression in memory B cells. *Blood* 101: 4500–4504. doi:[10.1182/blood-2002-11-3569](https://doi.org/10.1182/blood-2002-11-3569)
- Bibert S, Roger T, Calandra T, Bochud M, Cerny A, Semmo N, Duong FH, Gerlach T, Malinverni R, Moradpour D, et al (2013) IL28B expression depends on a novel TT/-G polymorphism which improves HCV clearance prediction. *J Exp Med* 210: 1109–1116. doi:[10.1084/jem.20130012](https://doi.org/10.1084/jem.20130012)
- Billerbeck E, Kang YH, Walker L, Lockstone H, Grafmueller S, Fleming V, Flint J, Willberg CB, Bengsch B, Seigel B, et al (2010) Analysis of CD161 expression on human CD8+ T cells defines a distinct functional subset with tissue-homing properties. *Proc Natl Acad Sci U S A* 107: 3006–3011. doi:[10.1073/pnas.0914839107](https://doi.org/10.1073/pnas.0914839107)
- Billiau A (2006) Anti-inflammatory properties of type I interferons. *Antiviral Res* 71: 108–116. doi:[10.1016/j.antiviral.2006.03.006](https://doi.org/10.1016/j.antiviral.2006.03.006)
- Blair PA, Norena LY, Flores-Borja F, Rawlings DJ, Isenberg DA, Ehrenstein MR, Mauri C (2010) CD19(+)/CD24(hi)CD38(hi) B cells exhibit regulatory capacity in healthy individuals but are functionally impaired in systemic Lupus Erythematosus patients. *Immunity* 32: 129–140. doi:[10.1016/j.immuni.2009.11.009](https://doi.org/10.1016/j.immuni.2009.11.009)
- Blazek K, Eames HL, Weiss M, Byrne AJ, Perocheau D, Pease JE, Doyle S, McCann F, Williams RO, Udalova IA (2015) IFN-lambda resolves inflammation via suppression of neutrophil infiltration and IL-1beta production. *J Exp Med* 212: 845–853. doi:[10.1084/jem.20140995](https://doi.org/10.1084/jem.20140995)
- Brenchley JM, Karandikar NJ, Betts MR, Ambrozak DR, Hill BJ, Crotty LE, Casazza JP, Kuruppu J, Migueles SA, Connors M, et al (2003) Expression of CD57 defines replicative senescence and antigen-induced apoptotic death of CD8+ T cells. *Blood* 101: 2711–2720. doi:[10.1182/blood-2002-07-2103](https://doi.org/10.1182/blood-2002-07-2103)
- Cooper S, Erickson AL, Adams EJ, Kansopon J, Weiner AJ, Chien DY, Houghton M, Parham P, Walker CM (1999) Analysis of a successful immune response against hepatitis C virus. *Immunity* 10: 439–449. doi:[10.1016/S1074-7613\(00\)80044-8](https://doi.org/10.1016/S1074-7613(00)80044-8)
- Curtsinger JM, Valenzuela JO, Agarwal P, Lins D, Mescher MF (2005) Type I IFNs provide a third signal to CD8 T cells to stimulate clonal expansion and differentiation. *J Immunol* 174: 4465–4469. doi:[10.4049/jimmunol.174.8.4465](https://doi.org/10.4049/jimmunol.174.8.4465)
- Das A, Ellis G, Pallant C, Lopes AR, Khanna P, Peppas D, Chen A, Blair P, Dusheiko G, Gill U, et al (2012) IL-10-producing regulatory B cells in the pathogenesis of chronic hepatitis B virus infection. *J Immunol* 189: 3925–3935. doi:[10.4049/jimmunol.1103139](https://doi.org/10.4049/jimmunol.1103139)
- de Groen RA, Groothuisink ZM, Liu BS, Boonstra A (2015) IFN-lambda is able to augment TLR-mediated activation and subsequent function of primary human B cells. *J Leukoc Biol* 98: 623–630. doi:[10.1189/jlb.3a0215-041rr](https://doi.org/10.1189/jlb.3a0215-041rr)
- Dickensheets H, Sheikh F, Park O, Gao B, Donnelly RP (2013) Interferon-lambda (IFN-lambda) induces signal transduction and gene expression in human hepatocytes, but not in lymphocytes or monocytes. *J Leukoc Biol* 93: 377–385. doi:[10.1189/jlb.0812395](https://doi.org/10.1189/jlb.0812395)
- Diepolder HM, Gerlach JT, Zachoval R, Hoffmann RM, Jung MC, Wierenga EA, Scholz S, Santantonio T, Houghton M, Southwood S, et al (1997) Immunodominant CD4+ T-cell epitope within nonstructural protein 3 in acute hepatitis C virus infection. *J Virol* 71: 6011–6019. doi:[10.1128/jvi.71.8.6011-6019.1997](https://doi.org/10.1128/jvi.71.8.6011-6019.1997)
- Donnelly RP, Sheikh F, Kotelko SV, Dickensheets H (2004) The expanded family of class II cytokines that share the IL-10 receptor-2 (IL-10R2) chain. *J Leukoc Biol* 76: 314–321. doi:[10.1189/jlb.0204117](https://doi.org/10.1189/jlb.0204117)
- Duong FH, Filipowicz M, Tripodi M, La Monica N, Heim MH (2004) Hepatitis C virus inhibits interferon signaling through up-regulation of protein phosphatase 2A. *Gastroenterology* 126: 263–277. doi:[10.1053/j.gastro.2003.10.076](https://doi.org/10.1053/j.gastro.2003.10.076)
- Egli A, Santer DM, O'Shea D, Barakat K, Syedbash M, Vollmer M, Baluch A, Bhat R, Groenendyk J, Joyce MA, et al (2014) IL-28B is a key regulator of B- and T-cell vaccine responses against influenza. *PLoS Pathog* 10: e1004556. doi:[10.1371/journal.ppat.1004556](https://doi.org/10.1371/journal.ppat.1004556)
- El-Serag HB (2012) Epidemiology of viral hepatitis and hepatocellular carcinoma. *Gastroenterology* 142: 1264–1273.e1. doi:[10.1053/j.gastro.2011.12.061](https://doi.org/10.1053/j.gastro.2011.12.061)
- Fergusson JR, Smith KE, Fleming VM, Rajoriya N, Newell EW, Simmons R, Marchi E, Bjorkander S, Kang YH, Swadlow L, et al (2014) CD161 defines a transcriptional and functional phenotype across distinct human T cell lineages. *Cell Rep* 9: 1075–1088. doi:[10.1016/j.celrep.2014.09.045](https://doi.org/10.1016/j.celrep.2014.09.045)
- Francisco LM, Sage PT, Sharpe AH (2010) The PD-1 pathway in tolerance and autoimmunity. *Immunol Rev* 236: 219–242. doi:[10.1111/j.1600-065x.2010.00923.x](https://doi.org/10.1111/j.1600-065x.2010.00923.x)
- Gallagher G, Megjugorac NJ, Yu RY, Eskdale J, Gallagher GE, Siegel R, Tollar E (2010) The lambda interferons: Guardians of the immune-epithelial interface and the T-helper 2 response. *J Interferon Cytokine Res* 30: 603–615. doi:[10.1089/jir.2010.0081](https://doi.org/10.1089/jir.2010.0081)
- Gil MP, Salomon R, Louten J, Biron CA (2006) Modulation of STAT1 protein levels: A mechanism shaping CD8 T-cell responses in vivo. *Blood* 107: 987–993. doi:[10.1182/blood-2005-07-2834](https://doi.org/10.1182/blood-2005-07-2834)
- Grakoui A, Shoukry NH, Woollard DJ, Han JH, Hanson HL, Ghayeb J, Murthy KK, Rice CM, Walker CM (2003) HCV persistence and immune evasion in the absence of memory T cell help. *Science* 302: 659–662. doi:[10.1126/science.1088774](https://doi.org/10.1126/science.1088774)
- Hahsler M, Piekenbrock M (2018) dbSCAN: Density based clustering of applications with noise (DBSCAN) and related algorithms.
- Hamming OJ, Terczynska-Dyla E, Vieyres G, Dijkman R, Jorgensen SE, Akhtar H, Siupka P, Pietschmann T, Thiel V, Hartmann R (2013) Interferon lambda 4 signals via the IFNlambda receptor to regulate antiviral activity against HCV and coronaviruses. *EMBO J* 32: 3055–3065. doi:[10.1038/emboj.2013.232](https://doi.org/10.1038/emboj.2013.232)

- Heim MH, Bochud PY, George J (2016) Host–hepatitis C viral interactions: The role of genetics. *J Hepatol* 65: S22–S32. doi:10.1016/j.jhep.2016.07.037
- Heim MH, Thimme R (2014) Innate and adaptive immune responses in HCV infections. *J Hepatol* 61: S14–S25. doi:10.1016/j.jhep.2014.06.035
- Hervas-Stubb S, Riezu-Boj JJ, Gonzalez I, Mancheno U, Dubrot J, Azpilicueta A, Gabari I, Palazon A, Aranguren A, Ruiz J, et al (2010) Effects of IFN-alpha as a signal-3 cytokine on human naive and antigen-experienced CD8(+) T cells. *Eur J Immunol* 40: 3389–3402. doi:10.1002/eji.201040664
- Huang Y, Blatt LM, Taylor MW (1995) Type 1 interferon as an antiinflammatory agent: Inhibition of lipopolysaccharide-induced interleukin-1 beta and induction of interleukin-1 receptor antagonist. *J Interferon Cytokine Res* 15: 317–321. doi:10.1089/jir.1995.15.317
- Jordan WJ, Eskdale J, Boniotto M, Rodia M, Kellner D, Gallagher G (2007a) Modulation of the human cytokine response by interferon lambda-1 (IFN-lambda1/IL-29). *Genes Immun* 8: 13–20. doi:10.1038/sj.gene.6364348
- Jordan WJ, Eskdale J, Srinivas S, Pekarek V, Kelner D, Rodia M, Gallagher G (2007b) Human interferon lambda-1 (IFN-lambda1/IL-29) modulates the Th1/Th2 response. *Genes Immun* 8: 254–261. doi:10.1038/sj.gene.6364382
- Kelly A, Robinson MW, Roche G, Biron CA, O'Farrelly C, Ryan EJ (2016) Immune cell profiling of IFN-lambda response shows pDCs express highest level of IFN-lambdaR1 and are directly responsive via the JAK-STAT pathway. *J Interferon Cytokine Res* 36: 671–680. doi:10.1089/jir.2015.0169
- Kotenko SV, Gallagher G, Baurin VV, Lewis-Antes A, Shen M, Shah NK, Langer JA, Sheikh F, Dickensheets H, Donnelly RP (2003) IFN-lambdas mediate antiviral protection through a distinct class II cytokine receptor complex. *Nat Immunol* 4: 69–77. doi:10.1038/ni875
- Kurioka A, Cosgrove C, Simoni Y, van Wilgenburg B, Geremia A, Bjorkander S, Sverremark-Ekstrom E, Thurnheer C, Gunthard HF, Khanna N, et al (2018) CD161 defines a functionally distinct subset of pro-inflammatory natural killer cells. *Front Immunol* 9: 486. doi:10.3389/fimmu.2018.00486
- Larbi A, Fulop T (2014) From “truly naive” to “exhausted senescent” T cells: When markers predict functionality. *Cytometry A* 85: 25–35. doi:10.1002/cyto.a.22351
- Lauer GM, Walker BD (2001) Hepatitis C virus infection. *N Engl J Med* 345: 41–52. doi:10.1056/nejm200107053450107
- Lechner F, Wong DK, Dunbar PR, Chapman R, Chung RT, Dohrenwend P, Robbins G, Phillips R, Klenerman P, Walker BD (2000) Analysis of successful immune responses in persons infected with hepatitis C virus. *J Exp Med* 191: 1499–1512. doi:10.1084/jem.191.9.1499
- Linderman GC, Rachh M, Hoskins JG, Steinerberger S, Kluger Y (2019) Fast interpolation-based t-SNE for improved visualization of single-cell RNA-seq data. *Nat Methods* 16: 243–245. doi:10.1038/s41592-018-0308-4
- Liu BS, Janssen HL, Boonstra A (2011) IL-29 and IFNalpha differ in their ability to modulate IL-12 production by TLR-activated human macrophages and exhibit differential regulation of the IFNgamma receptor expression. *Blood* 117: 2385–2395. doi:10.1182/blood-2010-07-298976
- Logvinoff C, Major ME, Oldach D, Heyward S, Talal A, Balfe P, Feinstone SM, Alter H, Rice CM, McKeating JA (2004) Neutralizing antibody response during acute and chronic hepatitis C virus infection. *Proc Natl Acad Sci U S A* 101: 10149–10154. doi:10.1073/pnas.0403519101
- Lund FE (2008) Cytokine-producing B lymphocytes-key regulators of immunity. *Curr Opin Immunol* 20: 332–338. doi:10.1016/j.coi.2008.03.003
- Mennechet FJ, Uze G (2006) Interferon-lambda-treated dendritic cells specifically induce proliferation of FOXP3-expressing suppressor T cells. *Blood* 107: 4417–4423. doi:10.1182/blood-2005-10-4129
- Missale G, Bertoni R, Lamonaca V, Valli A, Massari M, Mori C, Rumi MG, Houghton M, Fiaccadori F, Ferrari C (1996) Different clinical behaviors of acute hepatitis C virus infection are associated with different vigor of the anti-viral cell-mediated immune response. *J Clin Invest* 98: 706–714. doi:10.1172/jci118842
- Misumi I, Whitmire JK (2014) IFN-lambda exerts opposing effects on T cell responses depending on the chronicity of the virus infection. *J Immunol* 192: 3596–3606. doi:10.4049/jimmunol.1301705
- Mocsai A, Jakus Z, Vantus T, Berton G, Lowell CA, Ligeti E (2000) Kinase pathways in chemoattractant-induced degranulation of neutrophils: The role of p38 mitogen-activated protein kinase activated by Src family kinases. *J Immunol* 164: 4321–4331. doi:10.4049/jimmunol.164.8.4321
- Morrow MP, Pankhong P, Laddy DJ, Schoenly KA, Yan J, Cisneros N, Weiner DB (2009) Comparative ability of IL-12 and IL-28B to regulate Treg populations and enhance adaptive cellular immunity. *Blood* 113: 5868–5877. doi:10.1182/blood-2008-11-190520
- Nair S, Archer GE, Tedder TF (2012) Isolation and generation of human dendritic cells. *Curr Protoc Immunol* 7: 7.32. doi:10.1002/0471142735.im0732s99
- Negash AA, Ramos HJ, Crochet N, Lau DT, Doehle B, Papic N, Delker DA, Jo J, Bertolotti A, Hagedorn CH, et al (2013) IL-1beta production through the NLRP3 inflammasome by hepatic macrophages links hepatitis C virus infection with liver inflammation and disease. *PLoS Pathog* 9: e1003330. doi:10.1371/journal.ppat.1003330
- Neumann-Haefelin C, Thimme R (2013) Adaptive immune responses in hepatitis C virus infection. *Curr Top Microbiol Immunol* 369: 243–262. doi:10.1007/978-3-642-27340-7\_10
- Ng CT, Oldstone MB (2014) IL-10: Achieving balance during persistent viral infection. *Curr Top Microbiol Immunol* 380: 129–144. doi:10.1007/978-3-662-43492-5\_6
- Nguyen KB, Watford WT, Salomon R, Hofmann SR, Pien GC, Morinobu A, Gadina M, O'Shea JJ, Biron CA (2002) Critical role for STAT4 activation by type 1 interferons in the interferon-gamma response to viral infection. *Science* 297: 2063–2066. doi:10.1126/science.1074900
- Northfield JW, Kasprovicz V, Lucas M, Kersting N, Bengsch B, Kim A, Phillips RE, Walker BD, Thimme R, Lauer G, et al (2008) CD161 expression on hepatitis C virus-specific CD8+ T cells suggests a distinct pathway of T cell differentiation. *Hepatology* 47: 396–406. doi:10.1002/hep.22040
- Piscuoglio S, Lehmann FS, Zlobec I, Tornillo L, Dietmaier W, Hartmann A, Wunsch PH, Sessa F, Rummele P, Baumhoer D, et al (2012) Effect of EpCAM, CD44, CD133 and CD166 expression on patient survival in tumours of the ampulla of Vater. *J Clin Pathol* 65: 140–145. doi:10.1136/jclinpath-2011-200043
- Prokunina-Olsson L, Muchmore B, Tang W, Pfeiffer RM, Park H, Dickensheets H, Hergott D, Porter-Gill P, Mummy A, Kohaar I, et al (2013) A variant upstream of IFNL3 (IL28B) creating a new interferon gene IFNL4 is associated with impaired clearance of hepatitis C virus. *Nat Genet* 45: 164–171. doi:10.1038/ng.2521
- Rauch A, Kutalik Z, Descombes P, Cai T, Di Iulio J, Mueller T, Bochud M, Battegay M, Bernasconi E, Borovicka J, et al (2010) Genetic variation in IL28B is associated with chronic hepatitis C and treatment failure: A genome-wide association study. *Gastroenterology* 138: 1338–1345, 1345.e1–1345.e7. doi:10.1053/j.gastro.2009.12.056
- Read SA, Wijaya R, Ramezani-Moghadam M, Tay E, Schibeci S, Liddle C, Lam VWT, Yuen L, Douglas MW, Booth D, et al (2019) Macrophage coordination of the interferon lambda immune response. *Front Immunol* 10: 2674. doi:10.3389/fimmu.2019.02674
- Rivera A (2019) Interferon lambda's new role as regulator of neutrophil function. *J Interferon Cytokine Res* 39: 609–617. doi:10.1089/jir.2019.0036
- Rufer N, Zippelius A, Batard P, Pittet MJ, Kurth I, Cortesey P, Cerottini JC, Leyvraz S, Roosnek E, Nabholz M, et al (2003) Ex vivo characterization of human CD8+ T subsets with distinct replicative history and partial



- effector functions. *Blood* 102: 1779–1787. doi:[10.1182/blood-2003-02-0420](https://doi.org/10.1182/blood-2003-02-0420)
- Sallusto F, Lenig D, Forster R, Lipp M, Lanzavecchia A (1999) Two subsets of memory T lymphocytes with distinct homing potentials and effector functions. *Nature* 401: 708–712. doi:[10.1038/44385](https://doi.org/10.1038/44385)
- Santantonio T, Wiegand J, Gerlach JT (2008) Acute hepatitis C: Current status and remaining challenges. *J Hepatol* 49: 625–633. doi:[10.1016/j.jhep.2008.07.005](https://doi.org/10.1016/j.jhep.2008.07.005)
- Shoukry NH, Grakoui A, Houghton M, Chien DY, Ghrayeb J, Reimann KA, Walker CM (2003) Memory CD8+ T cells are required for protection from persistent hepatitis C virus infection. *J Exp Med* 197: 1645–1655. doi:[10.1084/jem.20030239](https://doi.org/10.1084/jem.20030239)
- Slifka MK, Whitton JL (2000) Antigen-specific regulation of T cell-mediated cytokine production. *Immunity* 12: 451–457. doi:[10.1016/s1074-7613\(00\)80197-1](https://doi.org/10.1016/s1074-7613(00)80197-1)
- Sommereyans C, Paul S, Staeheli P, Michiels T (2008) IFN-lambda (IFN-lambda) is expressed in a tissue-dependent fashion and primarily acts on epithelial cells in vivo. *PLoS Pathog* 4: e1000017. doi:[10.1371/journal.ppat.1000017](https://doi.org/10.1371/journal.ppat.1000017)
- Spagnuolo J (2018) FACKit: A FACS analysis toolkit.
- Srinivas S, Dai J, Eskdale J, Gallagher GE, Megjugorac NJ, Gallagher G (2008) Interferon-lambda1 (interleukin-29) preferentially down-regulates interleukin-13 over other T helper type 2 cytokine responses in vitro. *Immunology* 125: 492–502. doi:[10.1111/j.1365-2567.2008.02862.x](https://doi.org/10.1111/j.1365-2567.2008.02862.x)
- Takaki A, Wiese M, Maertens G, Depla E, Seifert U, Liebetrau A, Miller JL, Manns MP, Rehermann B (2000) Cellular immune responses persist and humoral responses decrease two decades after recovery from a single-source outbreak of hepatitis C. *Nat Med* 6: 578–582. doi:[10.1038/75063](https://doi.org/10.1038/75063)
- Terawaki S, Chikuma S, Shibayama S, Hayashi T, Yoshida T, Okazaki T, Honjo T (2011) IFN-alpha directly promotes programmed cell death-1 transcription and limits the duration of T cell-mediated immunity. *J Immunol* 186: 2772–2779. doi:[10.4049/jimmunol.1003208](https://doi.org/10.4049/jimmunol.1003208)
- Terczynska-Dyla E, Bibert S, Duong FH, Krol I, Jorgensen S, Collinet E, Kutalik Z, Aubert V, Cerny A, Kaiser L, et al (2014) Reduced IFNlambda4 activity is associated with improved HCV clearance and reduced expression of interferon-stimulated genes. *Nat Commun* 5: 5699. doi:[10.1038/ncomms6699](https://doi.org/10.1038/ncomms6699)
- Thimme R, Bukh J, Spangenberg HC, Wieland S, Pemberton J, Steiger C, Govindarajan S, Purcell RH, Chisari FV (2002) Viral and immunological determinants of hepatitis C virus clearance, persistence, and disease. *Proc Natl Acad Sci U S A* 99: 15661–15668. doi:[10.1073/pnas.202608299](https://doi.org/10.1073/pnas.202608299)
- Thimme R, Oldach D, Chang KM, Steiger C, Ray SC, Chisari FV (2001) Determinants of viral clearance and persistence during acute hepatitis C virus infection. *J Exp Med* 194: 1395–1406. doi:[10.1084/jem.194.10.1395](https://doi.org/10.1084/jem.194.10.1395)
- Thomas DL, Thio CL, Martin MP, Qi Y, Ge D, O’Huigin C, Kidd J, Kidd K, Khakoo SI, Alexander G, et al (2009) Genetic variation in IL28B and spontaneous clearance of hepatitis C virus. *Nature* 461: 798–801. doi:[10.1038/nature08463](https://doi.org/10.1038/nature08463)
- Tillmann HL, Thompson AJ, Patel K, Wiese M, Tenckhoff H, Nischalke HD, Lokhnygina Y, Kullig U, Gobel U, Capka E, et al (2010) A polymorphism near IL28B is associated with spontaneous clearance of acute hepatitis C virus and jaundice. *Gastroenterology* 139: 1586–1592. doi:[10.1053/j.gastro.2010.07.005](https://doi.org/10.1053/j.gastro.2010.07.005)
- Ussher JE, Bilton M, Attwod E, Shadwell J, Richardson R, de Lara C, Mettke E, Kurioka A, Hansen TH, Klenerman P, et al (2014) CD161++ CD8+ T cells, including the MAIT cell subset, are specifically activated by IL-12+IL-18 in a TCR-independent manner. *Eur J Immunol* 44: 195–203. doi:[10.1002/eji.201343509](https://doi.org/10.1002/eji.201343509)
- Wack A, Terczynska-Dyla E, Hartmann R (2015) Guarding the frontiers: The biology of type III interferons. *Nat Immunol* 16: 802–809. doi:[10.1038/ni.3212](https://doi.org/10.1038/ni.3212)
- West EE, Youngblood B, Tan WG, Jin HT, Araki K, Alexe G, Konieczny BT, Calpe S, Freeman GJ, Terhorst C, et al (2011) Tight regulation of memory CD8(+) T cells limits their effectiveness during sustained high viral load. *Immunity* 35: 285–298. doi:[10.1016/j.immuni.2011.05.017](https://doi.org/10.1016/j.immuni.2011.05.017)
- WHO (2017) *Global Hepatitis Report 2017*. Geneva: World Health Organization.
- Witte K, Gruetz G, Volk HD, Looman AC, Asadullah K, Sterry W, Sabat R, Wolk K (2009) Despite IFN-lambda receptor expression, blood immune cells, but not keratinocytes or melanocytes, have an impaired response to type III interferons: Implications for therapeutic applications of these cytokines. *Genes Immun* 10: 702–714. doi:[10.1038/gene.2009.72](https://doi.org/10.1038/gene.2009.72)
- Wood SN (2011) Fast stable restricted maximum likelihood and marginal likelihood estimation of semiparametric generalized linear models. *J R Stat Soc Ser B Stat Methodol* 73: 3–36. doi:[10.1111/j.1467-9868.2010.00749.x](https://doi.org/10.1111/j.1467-9868.2010.00749.x)
- Ye L, Schnepf D, Becker J, Ebert K, Tanriver Y, Bernasconi V, Gad HH, Hartmann R, Lycke N, Staeheli P (2019) Interferon-lambda enhances adaptive mucosal immunity by boosting release of thymic stromal lymphopoietin. *Nat Immunol* 20: 593–601. doi:[10.1038/s41590-019-0345-x](https://doi.org/10.1038/s41590-019-0345-x)



**License:** This article is available under a Creative Commons License (Attribution 4.0 International, as described at <https://creativecommons.org/licenses/by/4.0/>).